RESEARCH ARTICLE

Key Points:
- Large reservoirs of particulate and dissolved DMSP are present in the bottom ice
- Snowmelt and precipitation strongly influence DMSP releases from bottom ice
- Under-ice blooms produce high concentrations of DMSP

Correspondence to:
V. Galindo,
virginie.galindo@gmail.com

Biological and physical processes influencing sea ice, under-ice algae, and dimethylsulfoniopropionate during spring in the Canadian Arctic Archipelago

V. Galindo[1], M. Levasseur[1], C. J. Mundy[2], M. Gosselin[3], J.-É. Tremblay[1], M. Scarratt[4], Y. Gratton[5], T. Papakiriakou[2], M. Poulin[6], and M. Lizotte[1]

[1]Département de biologie, Québec-Océan, Université Laval, Québec, Québec, Canada, [2]Centre for Earth Observation Science, Faculty of Environment, Earth and Resources, University of Manitoba, Winnipeg, Manitoba, Canada, [3]Institut des sciences de la mer de Rimouski, Université du Québec à Rimouski, Rimouski, Québec, Canada, [4]Maurice Lamontagne Institute, Fisheries and Oceans Canada, Mont-Joli, Québec, Canada, [5]Institut National de Recherche Scientifique—Eau, Terre, et Environnement, Québec, Québec, Canada, [6]Research and Collections Division, Canadian Museum of Nature, Ottawa, Ontario, Canada

Abstract This study presents temporal variations in concentrations of chlorophyll a (Chl a), particulate and dissolved dimethylsulfoniopropionate (DMSPp and DMSPd) in the sea ice and underlying water column in the Canadian Arctic Archipelago during the spring of 2010 and 2011. During both years, bottom ice Chl a, DMSPp and DMSPd concentrations were high (up to 1328 µg L^{-1}, 15,082 nmol L^{-1}, and 6110 nmol L^{-1}, respectively) in May and decreased thereafter. The release of bottom ice algae and DMSPp in the water column was gradual in 2010 and rapid (8 days) in 2011. Bottom brine drainage during the presnowmelt period in 2010 and a rapid loss of the snow cover in 2011 coinciding with rain events explain most of the difference between the 2 years. During both years, less than 13% of the DMSPd lost from the ice was detected in the water column, suggesting a rapid microbial consumption. An under-ice diatom bloom developed in both years. In 2010, the bloom was dominated by centric diatoms while in 2011 pennates dominated, likely reflecting seeding by ice algae following the faster snowmelt progression induced by rainfall events in 2011. Both under-ice blooms were associated with high DMSPp concentrations (up to 185 nmol L^{-1}), but pennate diatoms showed DMSPp/Chl a ratios twice higher than centrics. These results highlight the key role of snowmelt and precipitation on the temporal pattern of ice-DMSP release to the water column and on the timing, taxonomic composition, and DMSP content of phytoplankton under-ice blooms in the Arctic.

1. Introduction

Dimethylsulfoniopropionate (DMSP) is the major biological precursor of the climate-active gas dimethylsulfide (DMS) [*Keller et al.*, 1989]. Close to 90% of biological fluxes of DMS originate from the marine environment [*Bates*, 1992; *Simó*, 2001]. In the atmosphere, oxidizing products of DMS can directly (as sulfate aerosols) and indirectly (as cloud condensation nuclei) reduce the amount of light reaching the Earth's surface, hence exerting a significant cooling impact on climate [*Charlson et al.*, 1987; *Andreae and Rosenfeld*, 2008]. The potential effect of oceanic emissions of DMS on climate has been recently challenged by *Quinn and Bates* [2011], but evidence of nucleation events linked to regional DMS ocean pulses shows that DMS can influence the dynamics of climate-active biogenic aerosols in remote regions [*Modini et al.*, 2009; *Chang et al.*, 2011; *Rempillo et al.*, 2011]. The impact of marine DMS emissions on local climate may be particularly important in the Arctic where warming is amplified by lower albedo due to the reduction of the summer ice cover [*Perovich et al.*, 2007; *Zhang et al.*, 2008; *Zhang*, 2010]. Modeling experiments suggest that the interaction between a larger ice-free sea surface available for gas exchange and a potential stimulation of biological DMS production could partly offset warming caused by the loss of ice albedo [*Gabric et al.*, 2005; *Qu and Gabric*, 2010].

DMSP is an abundant and widespread compound produced by several phytoplankton taxa [*Keller et al.*, 1989]. Cellular or particulate DMSP (DMSPp) has multiple roles. It can act as an osmoregulator [*Vairavamurthy et al.*, 1985; *Stefels*, 2000], an overflow mechanism for excess reduced sulfur under unbalanced growth

conditions [*Stefels*, 2000; *Stefels et al.*, 2007], a chemical defense against grazers [*Wolfe et al.*, 1997; *Steinke et al.*, 2002], and an antioxidant when algae are submitted to environmental stresses [*Matrai et al.*, 1995; *Sunda et al.*, 2002; *Archer et al.*, 2009]. Cellular DMSPp is released as dissolved DMSP (DMSPd) in the water as a result of cell lysis caused by grazing, viral attack, or autolysis [*Stefels*, 2000; *Simó*, 2001], and active exudation [*Laroche et al.*, 1999]. Heterotrophic bacteria usually maintain the DMSPd pool at a low level in the water column [*Simó*, 2001]. DMSPd can fulfill up to 13% of the bacterial carbon demand and up to 100% of their sulfur requirements [*Kettle and Andreae*, 2000; *Kiene et al.*, 2000; *Howard et al.*, 2006]. Both bacteria and some eukaryotic algae can synthesize different enzymes that cleave DMSP into DMS [*Stefels et al.*, 2007; *Curson et al.*, 2011; *Caruana et al.*, 2012; *Moran et al.*, 2012].

In polar regions, the vernal development of sea ice algae is accompanied by high concentrations of DMSP [*Levasseur et al.*, 1994; *Uzuka*, 2003; *Trevena and Jones*, 2006; *Tison et al.*, 2010], but the fate of this DMSP during the melt period is not well documented. In Antarctic waters, the release of sea ice DMSP has been suggested to be partially responsible for elevated DMSP concentrations in the water column at the ice edge during the melt period [*Kirst et al.*, 1991; *Curran and Jones*, 2000; *Trevena and Jones*, 2006; *Kiene et al.*, 2007; *Tison et al.*, 2010]. The release of ice algae and associated DMSP in the water column can result from brine drainage [*Lavoie et al.*, 2005; *Mundy et al.*, 2005] and ice melt [*Lizotte*, 2003; *Lavoie et al.*, 2005]. In addition, *Fortier et al.* [2002] observed that the release of ice algae in the water column can also be expedited by rain events. DMSP is present in particulate and dissolved phases in the sea ice and water column. Previous studies in polar regions only focused on total DMSP (i.e., DMSPt = DMSPp + DMSPd) due to the difficulty of sampling the dissolved phase. In contrast with DMSPp, which will likely sink rapidly in the water column, the ice-DMSPd pool is expected to remain in the fresh to brackish-water lens formed under the ice by meltwater. Both the size and fate of this ice-DMSPd pool are unknown.

The objectives of this study were to (1) characterize the temporal variations of the algal biomass, community composition, and DMSP (particulate and dissolved) in landfast first-year sea ice and in the water column during the melt period in the Canadian Arctic Archipelago, and (2) identify the mechanisms responsible for the release of chlorophyll *a* (Chl *a*) and DMSP from the ice into the water column.

2. Materials and Methods

2.1. Study Site

The study was conducted on landfast first-year sea ice in the central Canadian Arctic Archipelago during two consecutive vernal seasons as part of the Arctic-ICE (Ice Covered Ecosystem) project. Sampling took place in Resolute Passage (Station RP; water depth: 141 m) from 8 May to 21 June 2010 and in Allen Bay (Station AB; water depth: 60 m) from 8 May to 26 June 2011 (Figure 1). Samples were collected around 10:00 Central Daylight Time (UTC—05:00) on a 3 day schedule in 2010 and a 4 day schedule in 2011. The under-ice water column was sampled 1 day before the sea ice. Melt ponds covered the sea ice surface toward the end of both sampling years. The ice broke up between 12 and 16 July in 2010 and on 27 June in 2011.

2.2. Environmental Measurements

Air temperature was monitored at a meteorological station within 0.5–2 km of our main site (Vaisala, model HMP45C212 sensor) and surface albedo was calculated using the upwelling and downwelling shortwave radiation measurements from a four component net radiometer (Kipp & Zonen, model CNR1) installed at the station to describe the surface change and the transmitted irradiance through the ice over time. Daily rainfall data were provided by the Meteorological Service of Canada located in Resolute (ca. 7–10 km from the ice camps).

On each ice sampling day, snow depth and ice thickness were measured with a measuring stick and an ice thickness gauge (Kovacs Enterprises), respectively. Ice cores were extracted using a 9 cm internal diameter ice corer (Mark II Coring System, Kovacs Enterprises). Vertical profiles of temperature and salinity were determined on two full ice core sampled at a medium snow cover site at 13 and 12 occasions in 2010 and 2011, respectively. Ice temperature was measured at 5 cm intervals by drilling a 2 mm diameter hole to the center of the core and inserting a temperature probe (Testo 720 probe). To limit warming of the ice core, temperature measurements were done in the shade and as rapidly as possible (<20 min). To determine ice salinity,
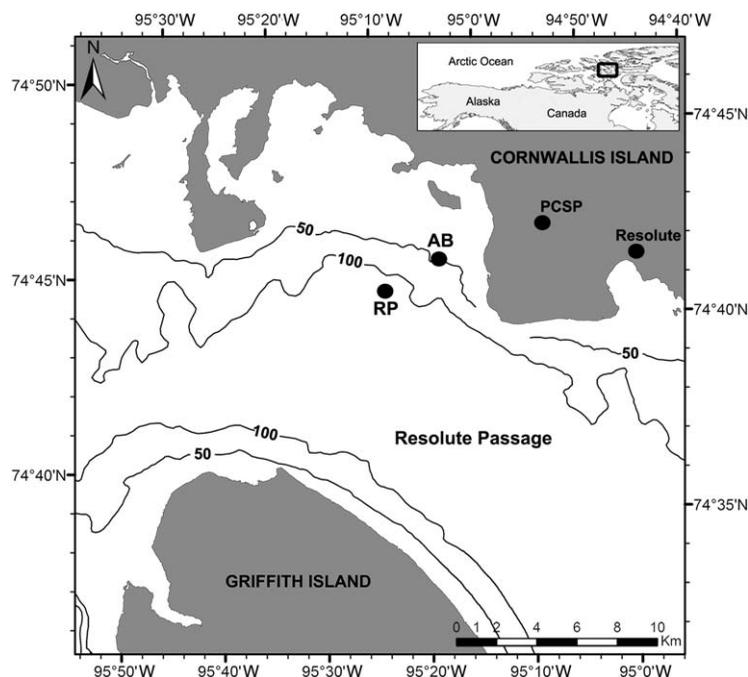
Figure 1. Map of the ice camp location in Resolute Passage (RP) in 2010 (74°42.6′N; 95°15′W) and in Allen Bay (AB) in 2011 (74°43′N 95°09′W). Locations of the hamlet of Resolute and of the Polar Continental Shelf Program (PCSP) Resolute Facility are also indicated. Isobaths are in meters.

the ice was cut at 10 cm intervals and melted. Bulk salinity of the melted ice was measured with a hand held conductivity meter (Cond 330i, WTW). Brine salinity and volume fraction of each 10 cm ice section were calculated using the recorded ice bulk salinity and temperature [*Cox and Weeks*, 1983; *Petrich and Eicken*, 2010].

Vertical profiles of temperature and salinity in the water column were measured with a Sea-Bird SBE 19plus V2 conductivity-temperature-depth (CTD) probe.

2.3. Sample Collection

Ice sampling was performed at low (<10 cm), medium (10–20 cm), and high (>20 cm) snow depth sites. At least two ice cores were extracted per site with the ice corer. The bottom 3 cm was quickly sectioned and pooled in a 7.5 L dark isothermal container to avoid brine drainage effects. These ice core samples were melted in 0.2 μm filtered seawater (three part FSW to one part melted ice) to minimize osmotic stress on the microbial community during melting [*Bates and Cota*, 1986; *Garrison and Buck*, 1986], and analyzed for Chl *a*, cell identification and enumeration, DMSPt and DMSPd. Two other ice cores were placed in sterile Nasco Whirl-Pak bags, and directly melted without FSW for analysis of total (brine and ice matrix) nutrients. The vertical distribution of Chl *a*, DMSPp and DMSPd was determined on full ice profiles at the medium snow cover sites on 12 occasions in 2010 (14, 17, 20, 24, 27, and 30 May, and 2, 6, 9, 12, 15, and 18 June) and four occasions in 2011 (10, 19, and 27 May, and 4 June). Ice cores were cut into sections starting with the bottom 3 cm, a 7 cm section, one 30 cm section, two 40 cm sections, and the top 20 cm in 2010, and in 2011 with the bottom 3 cm, a 7 cm section, one 40 cm section, one 60 cm section, and the top 40 cm.

Brine samples were collected by gravity using the sackhole brine sampling technique [*Thomas and Papadimitriou*, 2003]. On each brine sampling day, three holes of 20 cm diameter were drilled to depths of 60, 90, and 130 cm from the surface of the ice. The holes were covered with a high density Styrofoam cap. After 3 h, brines at the bottom of the holes were collected using a small electric submersible pump (12V Cyclone®) and kept in a 5 L Cubitainer in the dark until laboratory analysis.

Water column samples were collected at five depths in 2010 (2, 5, 10, 25, and 50 m below the sea surface) and in 2011 (2, 5, 10, 20, and 40 m below the sea surface) using 5 L Niskin bottles for the determination of nutrients, Chl *a*, protist cell identification and enumeration, and DMSPt and DMSPd.

2.4. Nutrients, Particulate Carbon, Algal Biomass, and Community Composition

Two subsamples for nutrient determination were filtered through a precombusted (5 h at 450°C) Whatman GF/F glass fiber filter inserted in a filter holder. The filtrate was collected into 15 mL acid-cleaned polyethylene tubes after thorough rinsing. Samples were immediately stored in a −20°C freezer until analysis of nitrate + nitrite (NOx hereinafter), phosphate, and silicic acid using standard colorimetric methods [*Grasshoff et al.*, 1999] adapted for the AutoAnalyzer 3 (SEAL Analytical) [*Martin et al.*, 2010]. The analytical detection limit for NOx, phosphate, and silicic acid were 0.03, 0.02, and 0.2 μmol L^{-1}, respectively.

To determine Chl *a* concentrations, two subsamples were filtered onto Whatman GF/F 25 mm filters. Pigments were extracted from the filters after a minimum of 18 h (maximum 24 h) in 90% acetone at 4°C in the dark [*Parsons et al.*, 1984]. Fluorescence of the extracted pigments was measured using a 10-005R Turner Designs fluorometer before and after acidification with 5% HCl. Chl *a* concentrations were calculated using the equation described by *Holm-Hansen et al.* [1965] and corrected for the dilution of the ice core section in FSW using the equation of *Cota and Sullivan* [1990].

Samples for the identification and enumeration of eukaryotic cells (>2 μm) were preserved with acidic Lugol's solution [*Parsons et al.*, 1984] and stored in the dark at 4°C until analysis. In the laboratory, at least 400 cells were enumerated using the inverted microscopy method [*Lund et al.*, 1958].

2.5. Determination of Dimethylated Sulfur Compounds

Duplicate sea ice and water column samples were collected for the determination of DMSPt and DMSPd. We used the ice melt technique [*Garrison and Buck*, 1986], which minimizes DMSP exudation due to osmotic shock. This melting technique may however have resulted in an underestimation of the particulate DMSP concentrations due to DMSP release in the dissolved phase and its subsequent bacterial conversion into DMS [*Stefels et al.*, 2012]. This bacterial conversion can be limited by the addition of 1.5% HCl during the melting of sea ice, as recently demonstrated by *Trevena and Jones* [2012]. *Stefels et al.* [2012] also discuss a new technique, the dry-crushing method, preventing the conversion of DMSP into DMS. These approaches should be favored in future studies to limit the exudation of DMSPd and its conversion into DMS during the melting period. For DMSPt, 3.5 mL of melted ice or seawater were collected into a 5 mL Falcon^{TM} tube, while DMSPd, which is notoriously difficult to measure, was quantified using the less disruptive Small-Volume gravity Drip Filtration (SVDF) method [*Kiene and Slezak*, 2006]. DMSP samples (3.5 mL) were preserved with 50 μL of 50% sulfuric acid (H$_2$SO$_4$). Samples were analyzed using a purge and trap system coupled to a Varian 3800 gas chromatograph (GC) equipped with a pulsed flame photometric detector (PFPD). The analytical detection limit was 0.01 nmol L^{-1} for all sulfur compounds.

To compare the distribution of sulfur compounds in different hydrographic regimes and the capacity of different algal groups and species to produce DMSP, DMSP concentrations were normalized to Chl *a* [e.g., *Turner et al.*, 1988; *Belviso*, 2000]. As for Chl *a*, sea ice DMSP concentrations were corrected for the dilution of ice core sections in FSW. Sea ice DMSPd concentrations were corrected for the presence of DMSPd in FSW using this equation:

$$C_{ICE} = (C_{BULK} \times V_{BULK} - C_{FSW} \times V_{FSW}) / V_{ICE} \qquad (1)$$

where C$_{ICE}$, C$_{BULK}$, and C$_{FSW}$ are the DMSPd concentrations (nmol L^{-1}) of the 3 cm bottom ice, the melted ice with FSW and the FSW used to melt the sea ice, respectively. V$_{ICE}$, V$_{BULK}$, and V$_{FSW}$ are the respective liquid volumes. Despite the addition of filtered seawater to minimize osmotic stress during the melting of ice, algal cells may have been stressed [*Hudier et al.*, 1995; *Mikkelsen and Witkowski*, 2010], resulting in a release of DMSPd in the samples. Therefore, we note that this technique may have slightly overestimated the DMSPd in the sea ice.

2.6. Statistical Analysis

Abiotic and biotic variables were tested for normality using the Shapiro-Wilk test with a 0.05 significance level. Relationships between variables were determined with Pearson's linear correlations (r). When the data were not normally distributed, Spearman's rank correlations (r$_s$) were used. Model II linear regressions (reduced major axis) [*Sokal and Rohlf*, 1995] were used to evaluate linear relationships between DMSPp and Chl *a* in the bottom ice and in the upper 50 m of the water column in both years. Regression slopes were
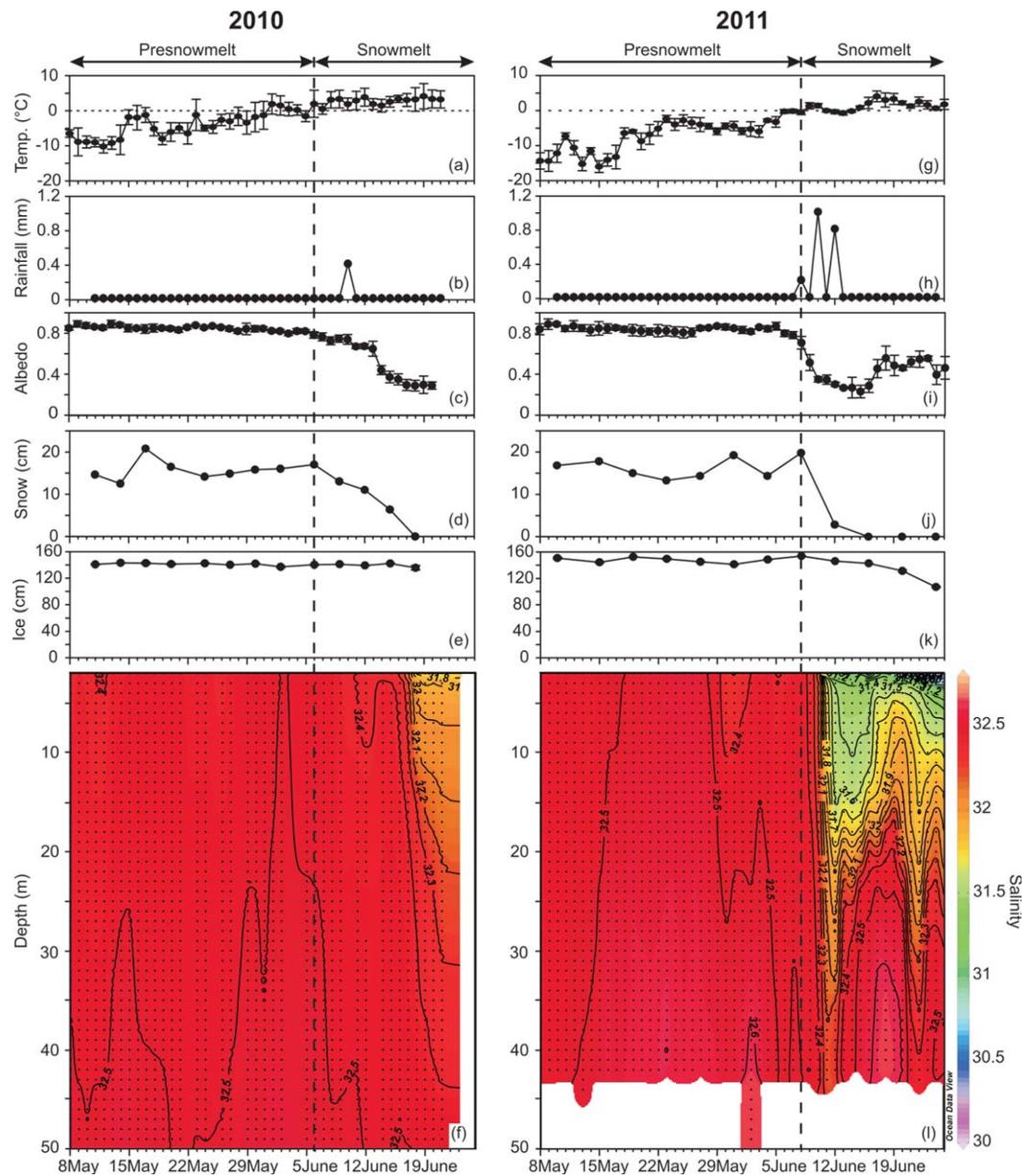
Figure 2. Time series of (a and g) daily averaged air temperature, (b and h) daily rainfall, (c and i) surface albedo, (d and j) site-averaged snow depth, (e and k) site-averaged ice thickness, and (f and l) salinity in the upper 50 m of the water column in Resolute Passage in 2010 and in Allen Bay in 2011, respectively. In Figures 2a, 2c, 2e, 2g, 2i, and 2k, bars represent standard deviation (SD). Vertical dashed lines indicate separation between the period before and during snowmelt.

compared using the analysis of covariance. Statistical differences between the two sampling years were tested using the Mann-Whitney test. Statistical tests were carried out using JMP® 10.0 software. Contour plots were drawn using a VG Gridding (a variable resolution grid using a weighted averaging scheme with the weights decreasing exponentially with distance) with Ocean Data view 4.0 software [*Schlitzer*, 2010] and graphics were produced with SigmaPlot 12.0 (Systat Software Inc.).

3. Results

3.1. Sea Ice and Oceanographic Conditions

In 2010, daily averaged air temperature increased progressively from $-7°C$ to $4°C$, with temperature exceeding $0°C$ after 6 June (Figure 2a). The sampling period was marked by a single small rain event on 10 June (Figure 2b).
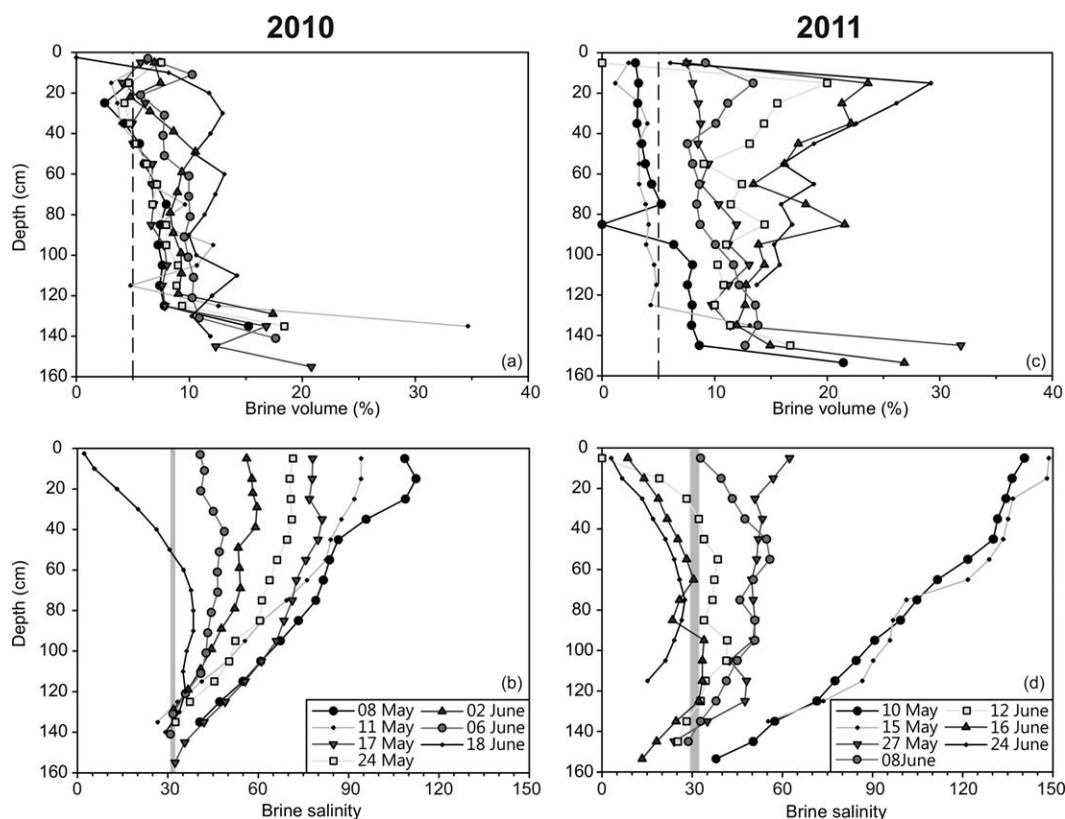
Figure 3. Time series of (a and c) brine volume fraction and (b and d) brine salinity at the medium snow cover site in Resolute Passage in 2010 and in Allen Bay in 2011, respectively. Vertical dashed lines in Figures 3a and 3c, and the gray bars in Figures 3b and 3d indicate 5% of brine volume and the range of surface seawater salinity, respectively.

Surface albedo remained relatively constant around 0.8 until 6 June, decreased slowly to 0.7 on 13 June due to snowmelt, and dropped down to 0.3 as a melt pond formed in the area (Figure 2c). Site-averaged snow depth remained relatively stable at 15 cm up to 6 June, then declined progressively to reach zero on 18 June (Figure 2d). Site-averaged sea ice thickness was constant at ca. 140 cm for the whole sampling period (Figure 2e). In 2010, the water column was relatively well mixed down to 50 m depth until 11 June when a 2–10 m lens of lower salinity developed at the ice-water interface as a result of the gradual melting of the snow cover (Figure 2f). The low-salinity lens deepened rapidly and reached ca. 30 m by the end of the sampling period.

In 2011, air temperature increased from $-14°C$ to $4°C$ during the entire sampling period and began to exceed $0°C$ on 8 June (Figure 2g). Two prominent and closely spaced rain events of 1 and 0.8 mm occurred on 10 and 12 June, respectively (Figure 2h). Surface albedo remained relatively constant around 0.8 until 6 June, and then decreased rapidly to 0.2 on 15 June due to the rain events and the formation of melt ponds (Figure 2i). Thereafter, the albedo increased to 0.6 due to the drainage of melt ponds and stayed relatively constant at this level until the end of the sampling period. Site-averaged snow depth was stable at around 15 cm until 8 June and decreased abruptly to reach 3 cm on 12 June during the rainy period (Figure 2j). Site-averaged sea ice thickness was constant at ca. 140 cm for most of the sampling period, but a significant loss of ice was observed toward the end of the sampling period (decreasing from 154 to 107 cm between 8 and 24 June; Figure 2k). In 2011, the water column exhibited the same salinity characteristics as in 2010 until the 10 June rainfall event which resulted in a rapid loss of the snow cover and a sharp decrease in surface salinity (from 32.5 to 31.8) down to 30 m (Figure 2l).

During both years, brine volume fractions were above 5% most of the time indicating a permeable sea ice cover [*Pringle et al.*, 2009], except at the beginning of the sampling in the upper 40 cm of the sea ice on 8 and 11 May 2010 (Figure 3a) and in the upper 80 cm of the sea ice on 10 and 15 May 2011 (Figure 3c). Brine volume fractions at the bottom of the ice in 2011 were not significantly different from 2010 ($p = 0.24$,
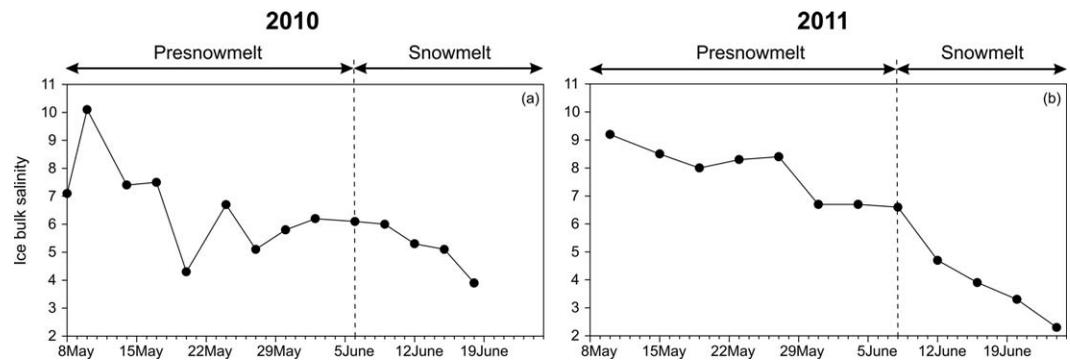
Figure 4. Time series of bulk salinity in the bottom 10 cm of the ice at the medium snow cover site (a) in Resolute Passage in 2010 and (b) in Allen Bay in 2011.

Mann-Whitney), with mean values of 21 $\pm$ 7% and 17 $\pm$ 6%, respectively. During the 2 years, the brine salinity in the bottom ice varied generally between 24 and 37 (Figures 3b and 3d), which is close to the salinity of the surface seawater (from 29 to 33, Figures 2f and 2l). Brine salinity sharply decreased on 18 June 2010 (upper 50 cm), 12 June 2011 (upper 30 cm), 16 June 2011 (most of the ice profile), and 24 June 2011 (full ice profile; Figures 3b and 3d).

In 2010, bulk salinity in bottom ice decreased from 10.1 to 5.1 between 10 and 27 May, and from 6.0 to 3.9 after 9 June (Figure 4a). In 2011, bulk salinity in bottom ice decreased more or less regularly from 9.5 to 2.3 during the whole sampling period, with a slightly faster decrease rate during the snowmelt period, after 8 June (Figure 4b).

In 2010, bottom sea ice temperature closely followed seawater temperature at 2 m below the sea surface during the most of the sampling period, except two sampling dates when the bottom ice temperature exceeded the temperature of the seawater (Figure 5a). Bottom sea ice temperatures in 2011 were higher than in 2010 ($p < 0.05$, Mann-Whitney) and were often warmer than the seawater temperature (Figure 5b).

3.2. Temporal Variations in NOx in Sea Ice and in the Water Column

The averaged concentrations of NOx measured in the bottom ice for the three snow depth sites and in the water column are presented in Figure 6. In 2010, NOx concentrations in bottom ice oscillated between 6 and 12 μmol L^{-1} from the beginning of the sampling until 2 June and then started to decrease progressively until the end of the sampling period (Figure 6a). NOx concentrations at 2 m below the sea surface showed the same trend as in the bottom ice with concentrations between 6 and 8 μmol L^{-1} during the
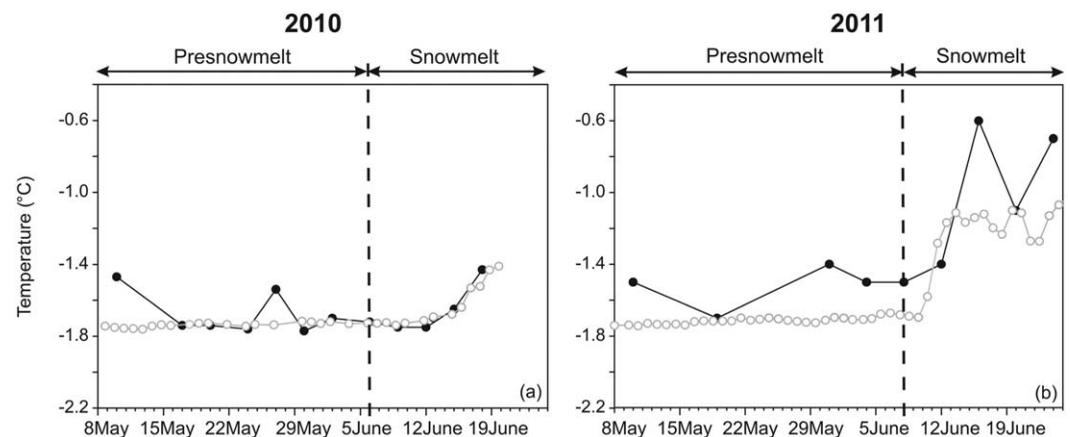

Figure 5. Time series of temperature of the 5 cm bottom ice (black closed circles) and at 2 m below the sea surface (gray open circles) (a) in Resolute Passage in 2010 and (b) in Allen Bay in 2011.
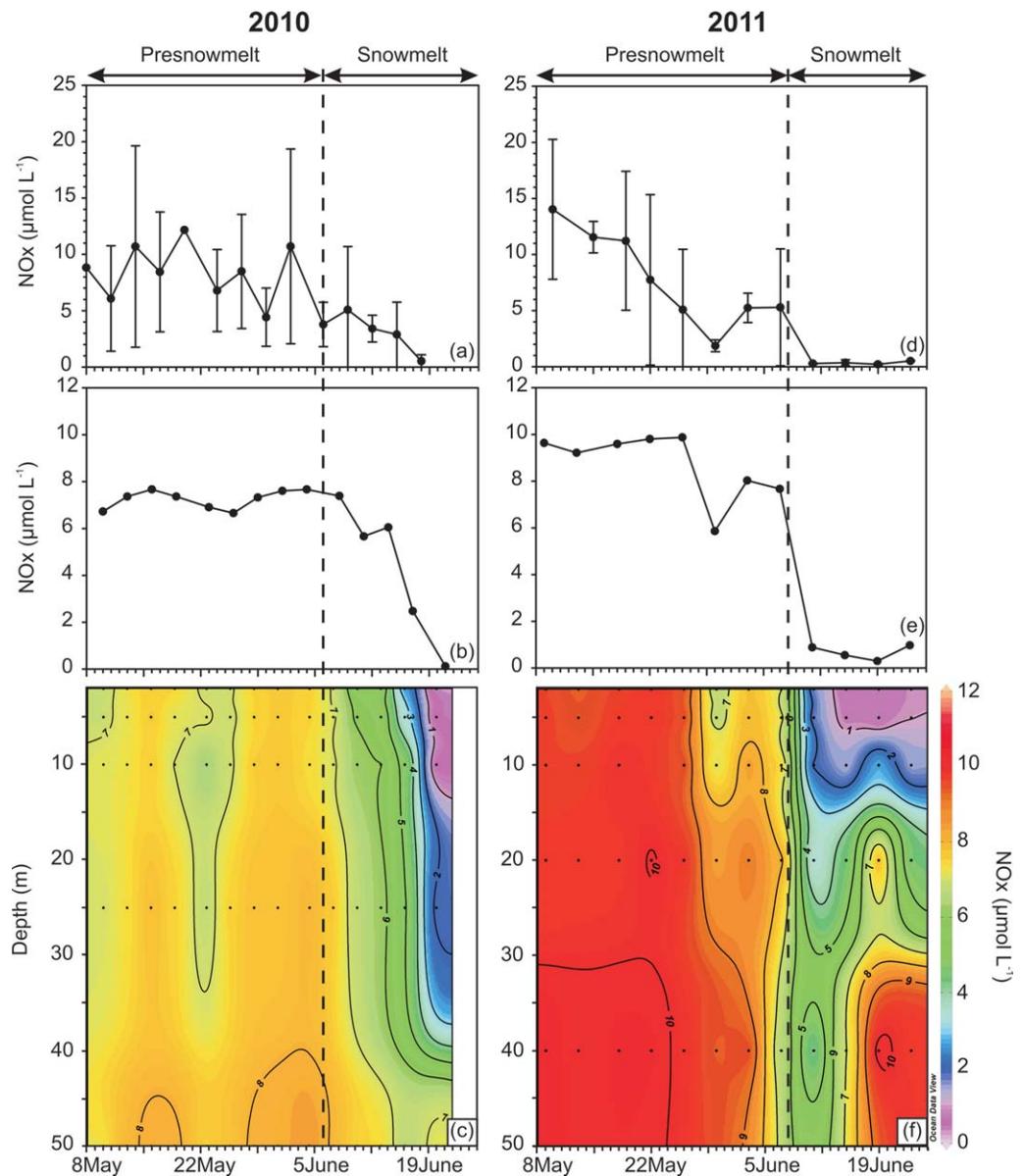
Figure 6. Time series of NOx concentrations (a and d) in the bottom 3 cm of the ice (mean ± SD), (b and e) at 2 m below the sea surface, and (c and f) in the upper 50 m of the water column in Resolute Passage in 2010 and in Allen Bay in 2011, respectively.

presnowmelt period and progressively decreasing values thereafter (Figure 6b). NOx concentrations in the upper 50 m of the water column decreased during the snowmelt period to a minimum of 0.6 μmol L^{-1} at 2 m on our last sampling day (Figure 6c). During the sampling period, concentrations of phosphate and silicic acid were always above 0.60 and 2.8 μmol L^{-1}, respectively, in the water column. Hence, nutrient concentrations were probably not limiting phytoplankton growth [*Mundy et al.*, 2014].

In 2011, NOx concentrations in bottom ice were initially 14 μmol L^{-1} and tended to decrease progressively down to 0.03 μmol L^{-1} (our detection limit) after 11 June (Figure 6d). A short-lived pulse of ca. 5 μmol L^{-1} was recorded on 3 and 7 June. As observed in the bottom ice, NOx concentrations in the upper 50 m of the water column were higher in 2011 than in 2010 at the beginning of the sampling (Figures 6e and 6f). At 2 m below the sea surface, NOx concentrations varied between 6 and 10 μmol L^{-1} until the rapid snowmelt period when they quickly decreased below 1 μmol L^{-1} (Figure 6e). The decrease in NOx concentrations
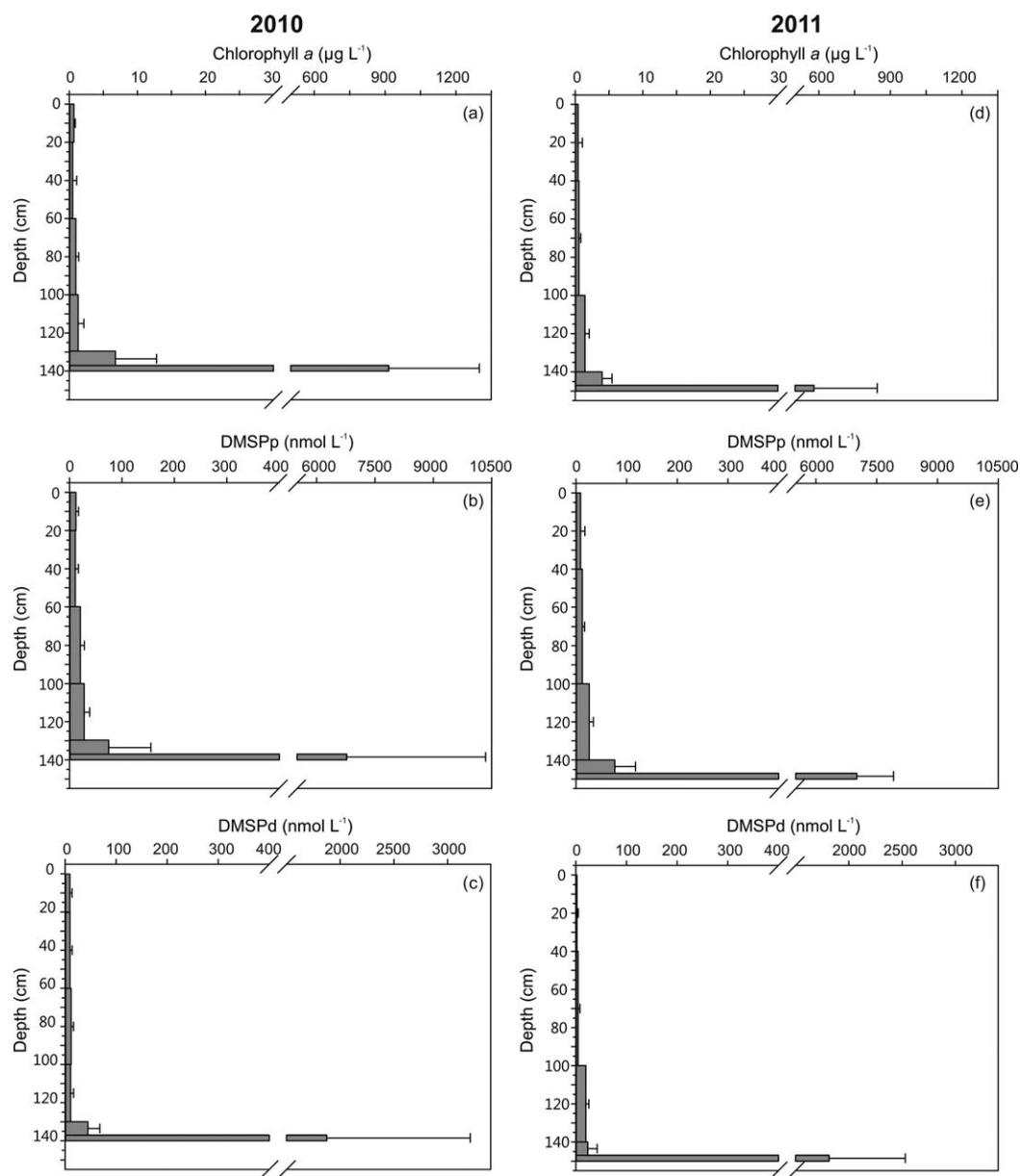
Figure 7. Vertical profiles of (a and d) chlorophyll *a*, (b and e) DMSPp, and (c and f) DMSPd concentrations in Resolute Passage in 2010 and in Allen Bay in 2011, respectively. Mean values ± SD bars are shown.

initiated on 27 May 2011 was observed down to 15 m in the water column (Figure 6f). As in 2010, phosphate and silicic acid concentrations in the water column were always above 0.51 and 1.5 μmol L^{-1} during the sampling period, respectively (data not shown). NOx concentrations in the bottom ice and at 2 m were positively correlated during both years (r = 0.64, $p < 0.05$ in 2010 and r_s = 0.79, $p < 0.01$ in 2011), suggesting an active nutrient exchange between the ice and the water column.

3.3. Vertical and Temporal Variations in Sea Ice and Water Column Chl a and DMSP

Concentrations of Chl *a*, DMSPp, and DMSPd in the different sea-ice horizons were averaged over the entire sampling period (Figure 7). During both years, Chl *a* and DMSP concentrations were mostly (>95%) concentrated in the bottom 3 cm of the ice core.

Figures 8 and 9 show the temporal variations of Chl *a*, DMSPp, and DMSPd in the bottom 3 cm of the ice and the upper 50 m of the water column in 2010 and 2011, respectively. The values of each bottom ice
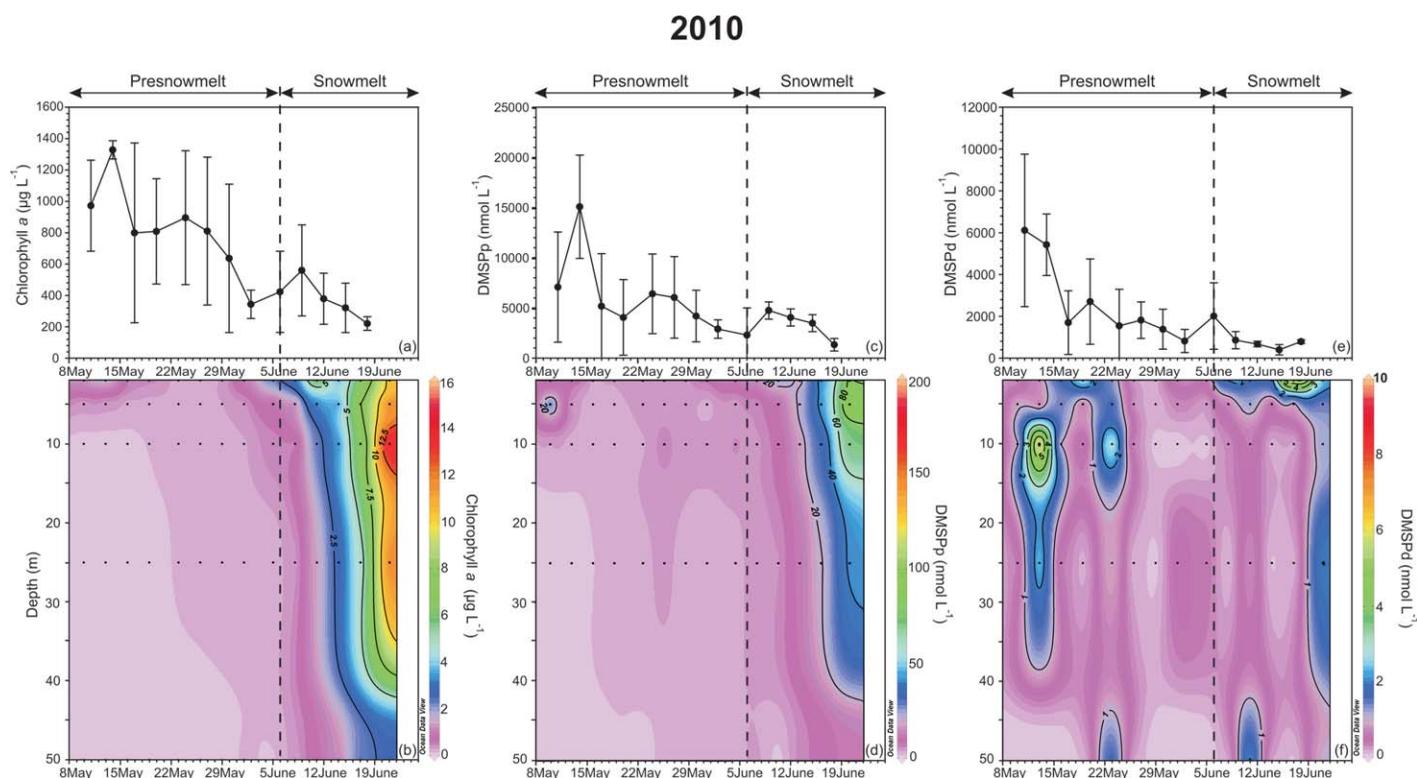
2010

Figure 8. Time series of (a and b) chlorophyll *a*, (c and d) DMSPp, and (e and f) DMSPd concentrations in the bottom 3 cm of the ice (mean ± SD) and the upper 50 m of the water column in Resolute Passage in 2010.

variable were averaged for the three snow depth sites. In 2010, bottom ice Chl *a* concentrations were above 1000 µg L^{-1} at the beginning of the sampling period (up to 1328 µg L^{-1} on the second sampling day) and decreased to reach a minimum value of 220 µg L^{-1} on our last sampling day (Figure 8a). Chl *a* concentrations in the under-ice water column were low in May (<0.25 µg L^{-1}), began to increase close to the surface on 6 June and reached a maximum value of 15.37 µg L^{-1} at 10 m on 21 June (Figure 8b). High Chl *a* concentrations were measured down to 35 m toward the end of the sampling period. DMSPp concentrations in the bottom ice showed a similar pattern as Chl *a* (r = 0.88, $p < 0.001$) with a peak value of 15,082 nmol L^{-1} measured during the second sampling day and a minimum value of 1329 nmol L^{-1} measured on the last sampling day (Figure 8c). In the water column, DMSPp concentrations were generally low (<7.5 nmol L^{-1}) from 10 to 29 May except the first value of 43 nmol L^{-1} measured on 10 May that was probably associated with sloughing of ice algae from the bottom ice prior to the start of our sampling (Figure 8d). A peak of 98 nmol L^{-1} was recorded on 21 June associated with development of the under-ice bloom. Bottom ice DMSPd concentrations were maximum at the beginning of the sampling in 2010 (6110 nmol L^{-1}), but decreased sharply on 17 May, and remained relatively constant at ca. 1700 nmol L^{-1} until 6 June when the concentrations fell below 800 nmol L^{-1} and remained low for the rest of the sampling period (Figure 8e). In the water column, DMSPd concentrations were often below the detection limit (<0.1 nmol L^{-1}) and generally lower than 5 nmol L^{-1} (Figure 8f). Two peaks of DMSPd were observed in 2010; one centered at 10 m at the beginning of the sampling period (13 May) and a second one at 2 m on 17 June. In both cases, these higher than average DMSPd concentrations extended down to ca. 40 m.

In 2011, bottom ice Chl *a* concentrations started at ca. 600 µg L^{-1}, remained relatively constant until 4 June, and then decreased sharply to become undetectable after 16 June (Figure 9a). In the water column, Chl *a* concentrations were below 0.5 µg L^{-1} at the beginning of the sampling period, increased to 4 µg L^{-1} on 30 May, reached a maximum value of 11 µg L^{-1} on 11 June, and started to decrease thereafter (Figure 9b). A subsurface chlorophyll maximum (SCM) began to form at the end of the sampling period. As in 2010, DMSPp
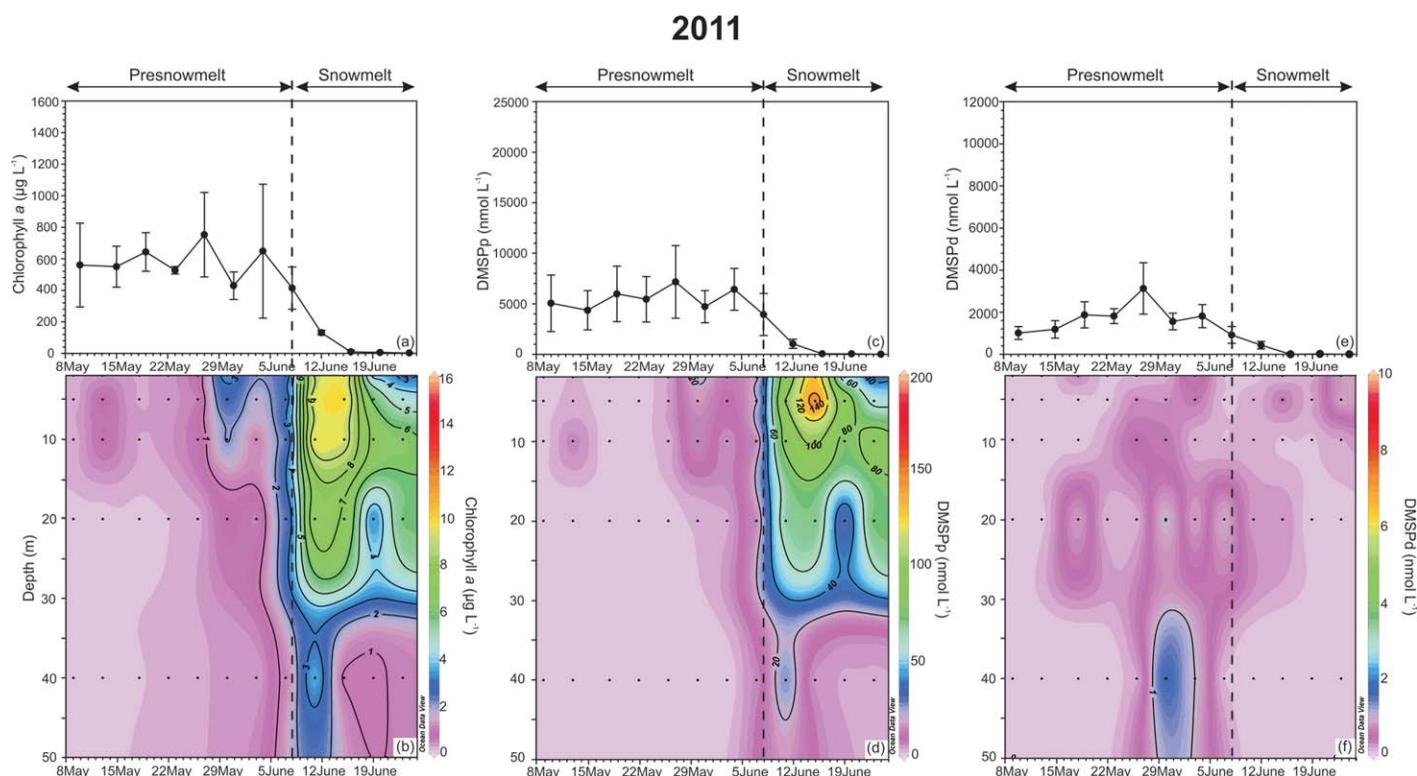
Figure 9. Time series of (a and b) chlorophyll *a*, (c and d) DMSPp, and (e and f) DMSPd concentrations in the bottom 3 cm of the ice (mean ± SD) and the upper 50 m of the water column in Allen Bay in 2011.

concentrations in the bottom ice were positively correlated with Chl *a* in 2011 (r = 0.99, *p* < 0.001). Bottom ice DMSPp concentrations varied between 4000 and 7000 nmol L^{-1} from the beginning of the sampling until 6 June, and then decreased rapidly (Figure 9c). In the water column, DMSPp concentrations were below 10 nmol L^{-1} at the beginning of the sampling period, started to increase on 30 May, and reached a maximum value of 185 nmol L^{-1} on 15 June (Figure 9d). DMSPd concentrations in the bottom ice were 1000 nmol L^{-1} at the beginning of the sampling, increased progressively to reach ca. 3000 nmol L^{-1} on 27 May, and then decreased to become undetectable after 20 June (Figure 9e). In the water column, DMSPd concentrations were low at the beginning of the sampling, reached a peak value of 2 nmol L^{-1} on 30 May, and decreased toward the end of sampling (Figure 9f).

During both years, DMSPp concentrations were strongly correlated with Chl *a* concentrations in the bottom ice (Figure 10a), and the slopes of the regressions were not significantly different between the 2 years (*p* = 0.16, covariance analysis). In contrast, the regression slopes between the DMSPp and Chl *a* concentrations in the upper 50 m of the water column were significantly different between the two sampling years (*p* < 0.0001, covariance analysis; Figure 10b).

3.4. Algal Abundance and Community Composition

High and low snow cover site averages of total cell abundance and relative abundance of the main protist taxa for selected sampling dates are presented in Figure 11. The taxonomic composition of the protist assemblage in the bottom ice was numerically dominated (60–80%) by pennate diatoms during both years. Major species were *Nitzschia frigida* Grunow (20–31% of pennate diatoms in 2010 and 22–51% in 2011) and *Navicula pelagica* Cleve (23–33% of pennate diatoms in 2010 and ca. 7% in 2011). Protist abundance in the bottom ice varied from 0.77×10^8 cells L^{-1} to 2.57×10^8 cells L^{-1} in 2010 and from 0.70×10^8 cells L^{-1} to 1.77×10^8 cells L^{-1} in 2011.

In the water column (ca. 0.5 m under the ice), the abundance of protists reached 3.4×10^6 cells L^{-1} in 2010 and 3.1×10^6 cells L^{-1} in 2011 at the peak of the under-ice phytoplankton blooms. The two under-ice
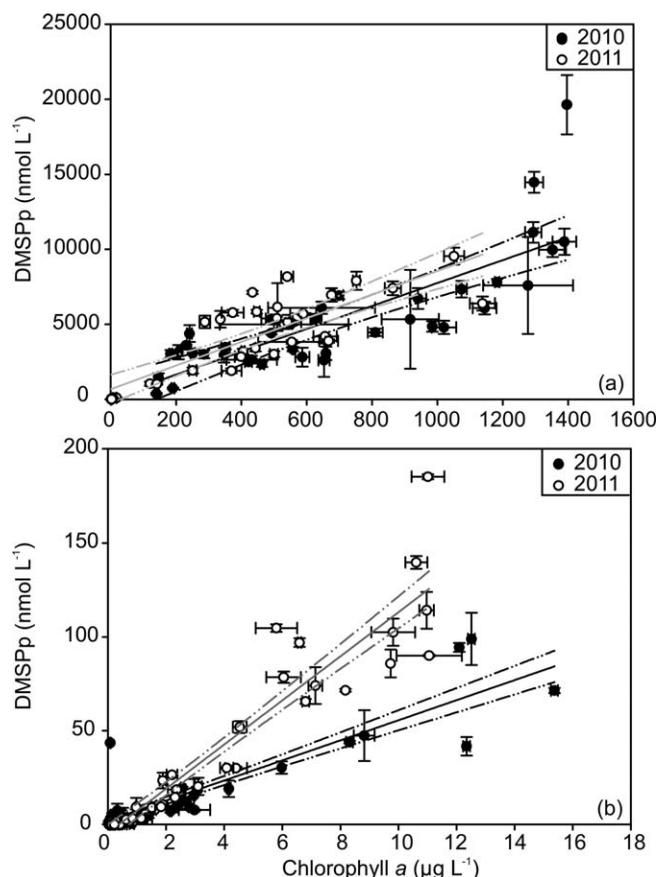
Figure 10. Relationships between DMSPp and chlorophyll a (a) in the bottom ice and (b) in the upper 50 m of the water column in Resolute Passage in 2010 (closed circles) and in Allen Bay in 2011 (open circles). Circles and horizontal/vertical lines represent mean and $\pm$SD, respectively. Model II linear regressions: (a) $x_2 = 9.50\,x_1 - 1054.67$, $r^2 = 0.88$, $p < 0.001$ (2010, closed circles, black line) and $x_2 = 9.36\,x_1 + 54.55$, $r^2 = 0.84$, $p < 0.001$ (2011, open circles, gray line), and (b) $x_2 = 5.89\,x_1 + 1.09$, $r^2 = 0.91$, $p < 0.001$ (2010, black line) and $x_2 = 12.40\,x_1 - 6.11$, $r^2 = 0.95$, $p < 0.001$ (2011, gray line). Dash-dot-lines represent the 95% confidence interval in black and gray for 2010 and 2011, respectively.

blooms exhibited different taxonomic compositions. In 2010, the prebloom community was heterogeneous until 14 June when centric diatoms started to increase in number (>65% of total protists). The dominant species during the under-ice bloom was *Chaetoceros socialis* Lauder (ca. 22–50% of centric diatoms). In 2011, the under-ice bloom was dominated by pennate diatoms (65% of total protists), which were represented by *Fossula arctica* Hasle, Syvertsen & von Quillfeldt (ca. 50–80%), *Fragilariopsis cylindrus* (Grunow ex Cleve) Frenguelli (ca. 2–19%), *Fragilariopsis oceanica* (Cleve) Hasle (ca. 2–15%), *Navicula septentrionalis* (Grunow) Gran (ca. 2–13%), and *Nitzschia frigida* (ca. 2%).

4. Discussion

4.1. Interannual Variability in Snow Cover and Water Column Stratification

For logistical reasons, it was impossible to occupy the exact same sampling location in 2010 and 2011. Although the two stations were closely located and exhibited similar sea ice type and thickness, some differences between the years reported here could reflect small-scale spatial heterogeneity. For instance, high spatial heterogeneity in the distribution of Chl a and DMSPt has also been reported in the fast ice of Prydz Bay in Antarctica by *Trevena et al.* [2003]. However, the two stations were sampled at the same time of the year and were subjected to similar solar irradiance. It is thus likely that the impact of environmental conditions on sea ice algae and under-ice blooms discussed hereafter reflects mostly interannual variability.

Different rainfall conditions encountered during the two sampling years led to distinct patterns of snow-melt, ice-algal release, and under-ice bloom development. In 2010, the gradual warming of the air, which exceeded 0°C on 6 June, caused a progressive melt of the snow cover which resulted in an increase in light transmittance through the ice as indicated by the decrease in surface albedo (Figure 2d) [*Mundy et al.*, 2014]. During that year, the sea ice became fully permeable after mid-May according to the threshold brine volume fractions of 5% (Figure 3a) [*Golden et al.*, 2007; *Vancoppenolle et al.*, 2007; *Pringle et al.*, 2009]. Freshening of surface waters was first observed on 11 June when snowmelt water likely drained through localized features in the ice cover including leads, seal holes, and possibly individual enlarged brine channels. This snowmelt drainage resulted in a decrease in seawater salinity from 32.5 to 31.8 at 4 m and a deepening of the 32 isohaline to 7 m at the end of the sampling period (Figure 2f). In 2011, air temperature first exceeded 0°C on 8 June, 2 days later than in 2010, but snow melting was accelerated by two rainfall events that occurred on 10 and 12 June (Figures 2g and 2j). The rapid snowmelt and the development of melt ponds observed around 8 June resulted in a sharp increase in light transmittance through the ice and coincided with a warming and melting of the bottom ice (Figures 2i–2k and 5b). Similar increases in light
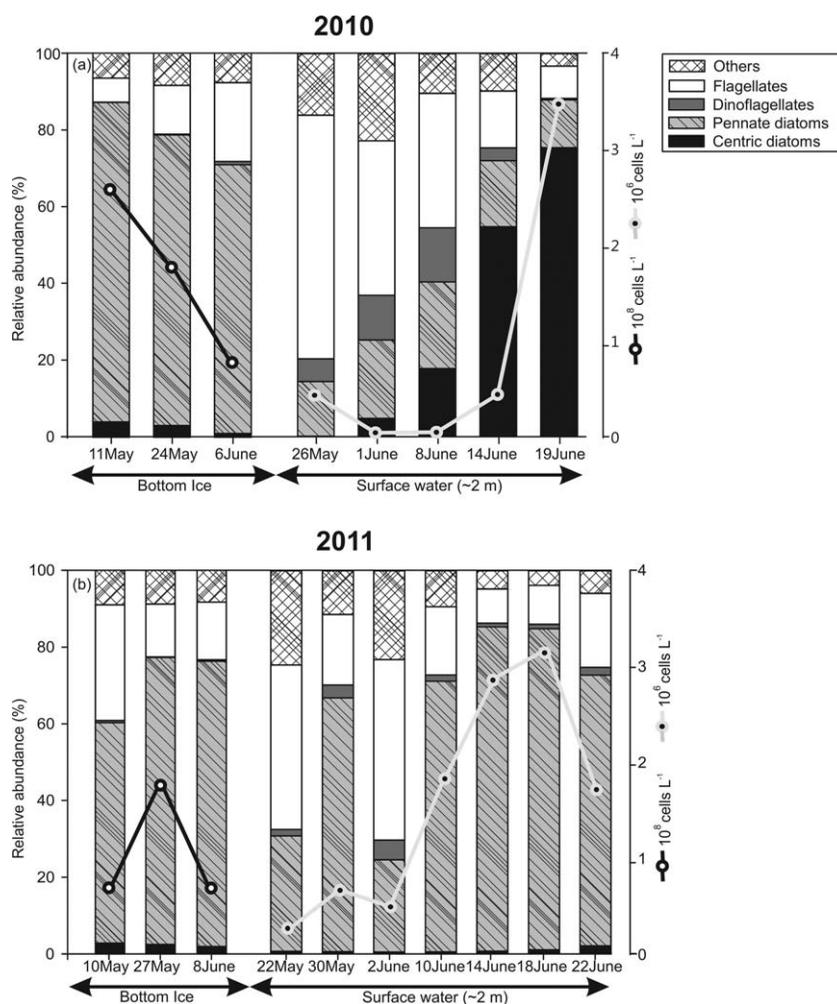
Figure 11. Temporal variations of relative (bar plot) and absolute cell abundance (line plot) of five groups of protists (a) in Resolute Passage in 2010 and (b) in Allen Bay in 2011. The group "Others" includes heterotrophic flagellates, ciliates, choanoflagellates, and unidentified cells.

transmittance through the sea ice due to the formation of melt ponds have been previously reported [*Ehn et al.*, 2011; *Frey et al.*, 2011; *Nicolaus et al.*, 2012]. Compared with 2010, the freshening of the upper water column was more important in 2011 with the 32 isohaline reaching 25 m toward the end of the sampling period (Figure 2l). As discussed in the following sections, these interannual variations influenced both the release pattern of the ice algae and its related DMSP in the water column and the subsequent development of the under-ice blooms.

4.2. Initial Biomass and Taxonomic Composition of the Sea Ice Algal Assemblages

During both years, we captured the peak and decline of the ice algal bloom as shown by the high Chl *a* (and DMSPp) measured at the beginning of the sampling period and the subsequent loss of ice algal biomass (Figures 8a and 9a). As observed during previous Arctic studies [*Smith et al.*, 1988; *Levasseur et al.*, 1994], the majority of Chl *a* (ca. 95 and 99%) and DMSPp (ca. 91 and 98%) was found in the last 3 cm of bottom ice in 2010 and 2011, respectively (Figures 6a, 6c, 6d, and 6f). Maximum integrated Chl *a* concentrations in the 3 cm bottom ice were 42 mg m^{-2} (1389 μg L^{-1}) in 2010 and 26 mg m^{-2} (864 μg L^{-1}) in 2011. These peak Chl *a* values are within the range of those reported in previous studies across the Arctic (2–340 mg m^{-2}) [e.g., *Arrigo et al.*, 2010]. However, they are at least three times lower than those reported by *Smith et al.* [1988] (225 mg m^{-2}) and *Levasseur et al.* [1994] (147 mg m^{-2}) in the same region during the spring of 1986 and 1992, respectively. Differences in snow thickness and nutrient concentrations in the water column (nitrate and silicic acid) could however not explain the lower sea ice algal biomass measured during our study.

Table 1. Concentrations of Total DMSP, Particulate DMSP, and Dissolved DMSP at the Bottom of the Sea Ice (BI) and in the Upper Water Column (WC) for Different Arctic Locations From the Literature and This Study

Location	Season	Environment	DMSPt (nmol L^{-1})	DMSPp (nmol L^{-1})	DMSPd (nmol L^{-1})	Source
Barents Sea	Winter	WC[a–c] (3 m)	3.2–16.8	1.5–10.3	0.5–6.3	*Matrai et al.* [2007]
	Spring		19–58.7	2.5–23.9	4.5–38.5	
	Summer		6.6–143.6	0.7–79.9	3.7–75.1	
Barrow, Alaska	Winter to Spring	BI (2 cm)	500–15,000			*Uzuka* [2003]
		WC[b] (5 m)	8–125			
Amundsen Gulf	Winter to Spring	BI (5 cm)	10–983			*Gilson* [2010]
Beaufort Sea	Winter to Spring	WC[b] (3 m)		1–4.3	<2.1	*Vila-Costa et al.* [2008]
Barents Sea	Spring	WC[a–c] (SL[d])		7–27	7–36	*Matrai and Vernet* [1997]
Northern Baffin Bay	Spring	BI (2 cm)		8.66–987		*Lee et al.* [2001]
		WC[b] (0–100 m)		0–9.53		
Northern Baffin Bay	Spring	WC[a] (SML[e])		0.02–1.35		*Lee et al.* [2003]
Northern Baffin Bay	Spring	BI (2 cm)		8.66–987	0.11–109	*Bouillon et al.* [2002]
		WC[b] (0–25 m)		0.09–9.53	0.02–11.8	
Resolute Passage	Spring	BI (5 cm)	0–6014			*Levasseur et al.* [1994]
		WC[b] (0–30 m)	8.25			
Resolute Passage	Spring	BI (2 cm)	28.52–729.38			*Levasseur* [2013]
		WC[b] (0–1 m)	4.22–85.80			
Resolute Passage	Spring	BI (3 cm)		1329–15,082	397–6110	This study
		WC[b] (0–50 m)		0.1–99	<9.32	
Allen Bay		BI (3 cm)		9.8–7162	0.6–3127	
		WC[b] (0–50 m)		lod[f]–185	<1.9	
Svalbard Archipelago	Spring to Summer	WC[a] (0–12 m)		10		*Archer et al.* [2013]
Svalbard Archipelago	Summer	WC[a] (0–150 m)		5–50	<2	*Damm et al.* [2008]
Greenland Sea	Summer	BI (20 cm)	90			*Gali and Simó* [2010]
		WC[a,b] (0–80 m)	1.4–163.6			
Bering Sea	Summer	WC[a] (SL[d])		10–80		*Lee et al.* [2011]
Central Arctic	Summer	WC[c] (SL[d])		4–26	3–7	*Matrai et al.* [2008]
Baffin Bay	Autumn	WC[a] (2–3 m)		8–39.2	<3	*Luce et al.* [2011]
Lancaster Sound		WC[a] (2–3 m)		15	<2	
Beaufort Sea		WC[a] (2–3 m)		2–17	<2	
Baffin Bay	Autumn	WC[a] (SL[d])		5–70	<1.7	*Motard-Côté et al.* [2012]
Lancaster Sound				10–23	<2.1	

[a]Open water.
[b]Ice-covered water.
[c]Ice-edge water.
[d]SL: surface layer.
[e]SML: surface mixed layer.
[f]lod: data below the limit of detection.

The ice algal community was numerically dominated by pennate diatoms (60–80% of total protists) during both years (Figure 11). The dominant species was *Nitzschia frigida* (20–31% and 22–51% of total pennate diatoms in 2010 and 2011, respectively), which is considered the sentinel species endemic in Arctic sea ice communities [*Poulin et al.*, 2011]. The remainder of the ice algal assemblage included other characteristic ice algae species such as *Navicula pelagica*, *Fragilariopsis cylindrus*, and *Fragilariopsis oceanica*.

4.3. Sea Ice Algal Biomass and Related DMSP

Concentrations of DMSPp in the bottom ice followed the same pattern as Chl *a*, reflecting a strong coupling between the processes responsible for the production and loss of these two compounds. Similar covariability between DMSPp and Chl *a* distribution in the sea ice has been reported for the Arctic [*Uzuka*, 2003] and the Antarctic [*Tison et al.*, 2010; *Nomura et al.*, 2011]. However, *Tison et al.* [2010] highlighted in Antarctic sea ice that this relationship may be lost when Chl *a* levels fall below 5 μg L^{-1}. As for Chl *a*, maximum bottom ice DMSPp concentrations were higher in 2010 (15,080 nmol L^{-1}) than in 2011 (7160 nmol L^{-1}). These bottom ice DMSP concentrations are within the range of values previously reported for the same region in spring [*Levasseur et al.*, 1994, bottom 5 cm] and in Barrow [*Uzuka*, 2003, bottom 2 cm], but higher than those previously measured in the northern part of Baffin Bay [*Lee et al.*, 2001, bottom 2 cm; *Bouillon et al.*, 2002, bottom 2 cm] and in the Amundsen Gulf [*Gilson*, 2010, bottom 5 cm] where lower algal biomasses were also observed (Table 1).

The slopes of the relationships between DMSPp and Chl *a* concentrations in the bottom ice were similar during the two sampling years (Figure 10a; 9.5 nmol DMSPp μg Chl *a*$^{-1}$ in 2010 and 9.4 nmol DMSPp μg

Chl a^{-1} in 2011), reflecting the prevailing similar ice algal assemblages. These DMSPp/Chl a ratios are low, as expected for this type of assemblage dominated by DMSP-poor diatoms. For sake of comparison, DMSPp/Chl a ratios of 790 and 171 nmol DMSPp µg Chl a^{-1} were measured during blooms of strong DMSP producers in the North Atlantic and North Pacific, respectively [*Scarratt et al.*, 2002; *Royer et al.*, 2010]. Nevertheless, due to the high biomass present, the bottom ice horizon represents a very rich DMSP environment. Indeed, the maximum stock of DMSPp measured in the 3 cm bottom ice during our study (453 µmol m^{-2}) represented ca. 20% of the DMSPp measured at the peak of the under-ice blooms in the upper 50 and 40 m of the water column in 2010 (2297 µmol m^{-2}) and in 2011 (2994 µmol m^{-2}), respectively.

4.4. Sea Ice Algal Biomass Declines

The two sampling years exhibited different temporal patterns of ice algal and DMSPp declines mostly related to snowmelt dynamics. In 2010, the decline was gradual and ice algae were still present at the bottom of the ice by the end of the sampling period (Figure 8a). During that year, variations in surface albedo were positively correlated with the thickness of the snow cover (r = 0.70, $p < 0.05$) as well as with the concentrations of Chl a at the bottom of the ice ($r_s = 0.90$, $p < 0.001$). Several nonexclusive mechanisms may explain a negative correlation between bottom ice algal biomass and light transmittance: (1) ice warming resulting from less thermal insulation from a thinner snow cover causing an increased heat flux and resulting in brine drainage [*Mundy et al.*, 2005], (2) additional warming of the bottom ice due to nonphotochemical quenching of light absorbed by ice algae [*Zeebe et al.*, 1996], and (3) negative physiological response of ice algae to light stress [*Barlow et al.*, 1988; *Michel et al.*, 1988; *Juhl and Krembs*, 2010; *Campbell et al.*, 2014]. In 2010, brine drainage took place during the presnowmelt period as indicated by the progressive decrease in bulk salinity in the bottom ice layer (Figure 4a). Toward the end of the sampling period, the increase in surface water and bottom ice temperatures suggest that warming of the bottom ice and associated loss of algal biomass could have been influenced by an enhanced ocean heat flux in addition to the increase of light transmittance (Figure 5a). Finally, the strong decrease in brine salinity over the upper ice column measured on the last sampling date in 2010 suggests ice desalination by flushing, i.e., the percolation of fresh meltwater through the permeable brine network [*Vancoppenolle et al.*, 2010].

In 2011, the decline of the ice algal biomass and its associated DMSPp was more abrupt (62% Chl a and 60% DMSPp lost in 8 days), closely following the increase in light transmittance resulting from the rapid, rain-induced, snowmelt (Figures 2h and 2j). These results suggest that the loss of biomass mostly resulted from the warming and melting of ice. This explanation is consistent with previous modeling work conducted in this region showing that the amount of light penetrating the snow cover can influence the decline of ice algal biomass through absorption and subsequent enhancement of the bottom ice melting rate [*Lavoie et al.*, 2005]. In addition, the decrease in bottom ice bulk salinity measured during this period indicates the presence of brine drainage (Figure 4b). Surface water temperature was generally colder than bottom ice temperature during these 8 days, indicating that ocean heat flux was not the main cause of bottom ice warming and melting (Figure 5b). The year 2011 was marked by a complete disappearance of ice algal biomass by the end of the sampling period, leaving a snow-free and quasi algae-free ice cover (Figure 9a). Although most of the ice melting took place after the major release event described before, ice melting may have also contributed to the removal of remaining ice algae at the end of the sampling period. The drastic decrease in brine salinity observed over the entire ice core between 12 and 24 June suggests that brine flushing due to hydrostatic pressure occurred at that time in 2011. Finally, the negative correlation between the bottom ice algal biomass and the under-ice current velocity calculated for 2011 (r = −0.62, $p < 0.05$), suggests that current erosion could have also contributed to the removal of ice algae (K. Campbell, personal communication, 2014).

Together, these results suggest that the loss of bottom ice algae during spring is controlled by a combination of factors including ice warming, brine drainage, flushing, and bottom ice erosion caused by currents. Our results suggest that difference in the patterns of algal biomass loss from the ice between 2010 and 2011 mostly resulted from the difference in wet precipitation between the two years. The acceleration of snow melting by the two rain events in 2011 enhanced ice warming and consequently ice melt that caused bottom ice Chl a to slough from the ice cover. Thus, in 2011, rainfalls caused a more rapid and almost complete termination of the ice algal bloom.

4.5. Sea Ice as a Source of Dissolved DMSP

Our results indicate the presence of a large reservoir of DMSPd in the bottom ice, with maxima of 6110 and 3127 nmol L^{-1} in 2010 and 2011, respectively. Before discussing further the potential importance of this
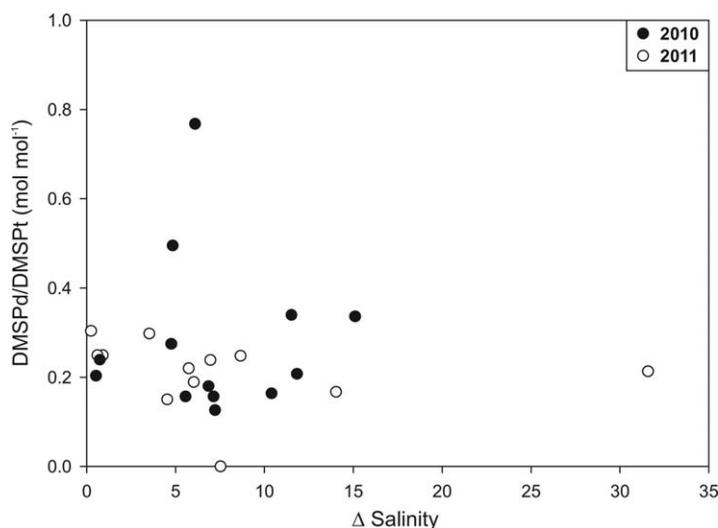
Figure 12. Relationships between the ratios of dissolved DMSP to total DMSP (DMSPd/DMSPt) and the change in salinity between the initial brine and the melted ice-FSW mixture (up to 27) at the end of the experimental melt period of the 3 cm bottom ice in Resolute Passage in 2010 (closed circles) and in Allen Bay in 2011 (open circles).

pool, the inherent and well-recognized difficulty of measuring dissolved DMSP needs to be addressed, especially in the sea ice. During sample processing and melt of the ice, ice algae can undergo a hypo-osmotic shock, which is difficult to totally suppress. Although the ice melt technique used in this study has been developed to minimize this osmotic shock [*Garrison and Buck*, 1986], ice algae are subjected to a rapid decrease in salinity that could result in DMSP exudation. To estimate the importance of this methodological artifact, we examined whether the DMSPd/DMSPt ratio showed a response to the change in salinity between the initial brine (up to 55) and the melted ice-FSW mixture (up to 27) at the end of the experimental melt period. Our calculations suggest that ice algae experienced an absolute change in salinity ranging from 0.2 to 32 during the melting process and no significant difference was observed among the DMSPd/DMSPt ratios (Figure 12). In addition, DMSPd concentrations measured in the bottom ice were in the range of expected values considering the high Chl *a* and DMSPp concentrations that prevail in this thin ice layer. Indeed, the maximum DMSPd/DMSPt ratio measured in the bottom ice (0.92 mol mol^{-1}) was comparable with the maximum ratio measured in the under-ice water column during this study (0.94 mol mol^{-1}; Table 2). Thus, we are confident that the thawing process and related potential osmotic shock did not significantly increase the measured DMSPd pool relative to DMSPp. However, as mentioned previously, this does not preclude a potential loss of DMSPd due to its bacterial conversion into DMS during the sea ice melting process.

In 2010, bottom ice DMSPd concentrations were extremely high at the beginning of the sampling period and showed a rapid decrease during the following week (Figure 8e). This rapid initial loss of DMSPd seems to be responsible for the increase in DMSPd concentrations in the upper 17 m of the water column (up to 3.61 nmol L^{-1}, Figure 8f). The importance of the ice-water column exchange of DMSPd was further explored by calculating how much DMSPd should have been measured in the water column following this release

Table 2. Concentrations of Total DMSP (DMSPt) and Dissolved DMSP (DMSPd), and Ratios of DMSPd/DMSPt From Sea Ice Cores, Sea Ice Brines, and the Water Column Underneath the Sea Ice in Resolute Passage in 2010[a]

Site	Depth (m)	DMSPt (nmol L^{-1})	DMSPd (nmol L^{-1})	DMSPd/DMSPt (mol mol^{-1})
Sea ice[b]	0–1.4	1149.08 ± 3094.43 (8.13–20,504.55)	291.43 ± 819.61 (3.81–5422.01)	0.36 ± 0.15 (0.10–0.92)
Sea ice brines[c]	0.6	53.65 ± 9.16 (40.96–72.89)	3.63 ± 1.00 (2.77–5.64)	0.07 ± 0.02 (0.06–0.11)
	0.9	50.94 ± 5.12 (45.09–60.47)	4.68 ± 0.82 (3.35–5.81)	0.09 ± 0.01 (0.07–0.11)
	1.3	37.90 ± 12.56 (24.80–60.67)	4.54 ± 1.00 (3.00–5.82)	0.13 ± 0.06 (0.08–0.23)
Water column[d]	0–50	13.80 ± 21.34 (0.70–99.97)	1.19 ± 3.41 (lod[e]–3.61)	0.21 ± 0.80 (0.0003–0.94)

[a]Mean ± SD and range (in parentheses) are shown for each sampling site.
[b]Sampling date: 14, 17, 20, 24, 27, and 30 May, and 2, 6, 9, 12, 15, and 18 June.
[c]Sampling date: 14, 17, 20, 24, 27, and 30 May, and 2 and 6 June.
[d]Sampling date: 7, 10, 13, 16, 19, 23, 26, and 29 May, and 1, 5, 8, 11, 14, 17, and 21 June.
[e]lod: Data below the limit of detection.

event in the absence of bacterial uptake. To do so, bulk-ice DMSPd concentrations were first converted to brine DMSPd concentrations following the method described for DMSP by *Tison et al.* [2010], which consists of multiplying the bulk-ice DMSP by the density value of 0.91 for first-year sea ice [*Timco and Frederking*, 1996] and dividing by the corresponding brine volume fraction. Then we calculated the theoretical vertically integrated DMSPd concentrations in the surface mixed layer assuming a complete flushing of bottom ice brine into the water column. Most of the ice-DMSPd is missing from the water column based on this calculation, the increase in DMSPd integrated over the upper 50 m of the water column amounting to only 3% of the DMSPd lost from the ice. It should be noted that the salinity field was fairly homogenous in the entire water column during the sampling period (Figures 2f and 2l), with no evidence of brine sinking as observed by *Jones et al.* [2010] on the Antarctic Shelf. Thus, microbial consumption is the most likely explanation for the missing DMSPd. To further explore this hypothesis, we calculated the turnover time of the DMSPd pool using a DMSPd microbial uptake rate of 8.8 nmol L^{-1} d^{-1} measured underneath the ice in the same area and period in 2012 (V. Galindo, unpublished data, 2014). We estimated that bacteria could have consumed all the DMSPd released from the ice during the 2010 release events in less than 2 days. Given our sampling interval of 3 days, bacterial consumption may thus explain the loss of DMSPd from the water column.

In 2011, the temporal pattern of bottom ice DMSPd exhibited a bell shape with a peak concentration of 3127 nmol L^{-1} measured on 27 May (Figure 9e). Due to the lack of DMSPd rate measurements in the ice, we cannot explain the increase in DMSPd concentrations in the bottom ice until 27 May. Based on the same calculations as in 2010, we estimated that the changes in DMSPd concentrations in the upper 40 m of the water column measured between 27 and 31 May could explain only 13% of the DMSPd lost from the ice during the same period. Our calculations of bacterial uptake suggest that bacteria present in the water column under the ice at this time of the year would have taken less than a day to consume the DMSPd released from the ice.

These results suggest the presence of a large reservoir of DMSPd in the bottom ice that appears to be rapidly metabolized by heterotrophic bacteria once released to the underlying water column. The exact size of this reservoir in the ice and how much of this ice-DMSPd is eventually cleaved to DMS and ventilated to the atmosphere or oxidized to dimethylsulfoxide (DMSO) still needs to be determined.

4.6. Under-Ice Blooms and Associated DMSP

During both years, an under-ice phytoplankton bloom accompanied by a NOx drawdown was observed in the water column toward the end of June (Figures 6b and 6e). Maximum Chl *a* concentrations of 15 μg L^{-1} and 11 μg L^{-1} were reached on 21 June 2010 (last sampling day) and 15 June 2011, respectively. These concentrations are similar to those normally measured in open water blooms or at ice-edge blooms in the Arctic [*Matrai and Vernet*, 1997; *Arrigo and van Dijken*, 2004; *Mundy et al.*, 2009]. Chl *a* concentrations were negatively correlated with salinity (r_s = -0.75 and -0.87 in 2010 and 2011, $p < 0.001$, respectively) as well as with sea ice albedo (r_s = -0.78, $p < 0.001$ in 2010 and -0.66, $p < 0.05$ in 2011). These correlations suggest that the blooms were linked to the development of the under-ice fresh to brackish-water lens resulting from the melting of snow and ice covers and the increase in light transmission through the ice.

Both the timing and taxonomic composition of the under-ice blooms were affected by the environmental conditions and snowmelt dynamics that characterized the 2 years. In 2010, the phytoplankton bloom started on 7 June based on the onset of NOx drawdown in the water column, which coincided with the beginning of the snowmelt period. The bloom was composed of centric diatoms with a dominance of *Chaetoceros* spp., a common late spring-summer species in Arctic waters [*von Quillfeldt*, 2000; *Poulin et al.*, 2011]. The under-ice bloom developed until at least 21 June, our last sampling day. This presumably corresponded closely to the bloom's apogee judging from the very low concentrations of NOx remaining in the upper water column [*Mundy et al.*, 2014].

In 2011, the under-ice bloom was initiated on the same date (7 June) as in 2010, when the snow started to melt, but reached its maximum biomass one week earlier (15 June versus 21 June in 2010), most probably due to the acceleration of snowmelt caused by the rain events. In contrast with 2010, the 2011 under-ice bloom was dominated by pennate diatoms, including *Fossula arctica*, *Fragilariopsis cylindrus*, *Fragilariopsis oceanica*, and *Nitzschia frigida* (up to 80%, 19%, 15%, and 2%, respectively, of total pennate diatoms), four species regularly found in early spring in the Arctic [*Grøntved and Seidenfaden*, 1938; *von Quillfeldt*, 2000]. *Fragilariopsis cylindrus*, *F. oceanica*, and *N. frigida* are considered sympagic and/or strikingly associated taxa with Arctic sea ice [*Poulin et al.*, 2011]. The dominance of pennate diatoms and the presence of sympagic algae in the under-ice bloom in 2011 suggest a seeding effect possibly linked to the rapid occurrence of

snowmelt. In 2011, the pelagic bloom developed rapidly and reached its declining phase under the ice as shown by decreasing Chl a concentrations in surface waters as well as the early development of a SCM. SCM are ubiquitous in the Arctic Ocean [*Tremblay et al.*, 2008; *Martin et al.*, 2010; *Popova et al.*, 2010], and our results reinforce the previous report of an under-ice SCM by *Arrigo et al.* [2012] in the Chukchi Sea.

The under-ice blooms were associated with high concentrations of DMSPp. The maximum DMSPp concentrations measured in the water column under the ice in 2010 (99 nmol L^{-1}) and in 2011 (185 nmol L^{-1}) are the highest concentrations ever measured in Arctic waters during the spring period (Table 1). As for Chl a, DMSPp concentrations in the water column were negatively correlated with salinity ($r_s = -0.70$ and -0.78 in 2010 and 2011, $p < 0.001$, respectively) and surface albedo ($r_s = -0.67$, $p < 0.01$ and -0.56, $p < 0.05$ in 2010 and 2011, respectively). Interestingly, the two under-ice blooms exhibited different DMSPp/Chl a ratios (Figure 10b; slope 5.89 nmol DMSPp μg Chl a^{-1} 2010 and 12.40 nmol DMSPp μg Chl a^{-1} in 2011). Under cold culture conditions, *Kasamatsu et al.* [2004] showed that the psychrophilic centric diatom *Chaetoceros* sp. has a lower DMSP quota than the pennate diatoms *Nitzschia* sp. and *Navicula* sp. The shift in dominance from centric (2010) to pennate diatoms (2011) may explain the higher DMSP/Chl a ratios observed in 2011.

5. Conclusion

During this study spanning two successive years (2010, 2011), we captured the decline of ice algae and the following development of under-ice phytoplankton blooms and their associated DMSP at two adjacent stations located in the Canadian Arctic Archipelago. Despite the dominance of DMSP-poor diatoms in the bottom ice, DMSPp concentrations were very high (up to 15,000 nmol L^{-1}) and represented the highest values recorded so far in Arctic sea ice. The release of bottom ice algae and its associated DMSPp in the water column exhibited two different patterns during the sampling years. In 2010, the loss of ice algae and DMSPp began during the presnowmelt period, with release events linked to bottom ice brine drainage. During the following snowmelt period, the loss of the remaining ice algae and DMSPp coincided with the warming of the bottom ice due to higher light transmittance and potentially an enhanced ocean heat flux. In 2011, the loss of ice algae and DMSPp was rapid (8 days) and coincided with two successive rain events and the rapid loss of the snow cover which resulted in the warming and melting of bottom ice and increase in brine drainage due to higher light transmittance. During both years when the snow cover had completely melted, flushing meltwater moved vertically through the ice as reported in *Griewank and Notz* [2014] and subsequently leached the brine channels. Our results also revealed the presence of a large reservoir of DMSPd in the bottom ice, with concentrations up to 6110 nmol L^{-1}. Quantifying DMSPd in sea ice is technically challenging, so these values should be considered as provisional even with the level of cautious handling and verification achieved. Our results suggest that most of this ice-DMSPd is consumed by bacteria once released into the water column where it could be potentially converted to DMS. During both years, melting of the snow cover and related increases in light transmittance and water column stratification favored the development of an under-ice phytoplankton bloom. DMSPp concentrations associated with these under-ice blooms were among the highest reported for Arctic seawater. Considering that the extent of these under-ice blooms are predicted to increase in the future [*Mundy et al.*, 2009; *Arrigo et al.*, 2012; *Boetius et al.*, 2013; *Matrai and Apollonio*, 2013], their importance as a source of DMSP and DMS needs to be further evaluated. Altogether, our results confirm the importance of Arctic sea ice as a source of DMSPp, and potentially DMSPd and DMS, for the water column during spring. Furthermore, rain, which has been predicted to intensify under a warmer climate [*White et al.*, 2007; *Rawlins et al.*, 2010], accelerated snow melting in 2011 and resulted in a snow-free, nearly algae-free, and highly transparent ice cover. These conditions led to the rapid development of an under-ice bloom dominated by pennate sympagic diatoms in contrast with the under-ice bloom dominated by centric pelagic diatoms in 2010. DMSP production was also higher in the 2011 pennate diatom bloom than in the 2010 centric bloom. These results suggest that the projected increase in rainfall during the spring period due to climate warming could favor the development of DMSP-rich under-ice blooms dominated by pennate diatoms.

References

Andreae, M. O., and D. Rosenfeld (2008), Aerosol–cloud–precipitation interactions. Part 1. The nature and sources of cloud-active aerosols, *Earth Sci. Rev.*, *89*(1–2), 13–41, doi:10.1016/j.earscirev.2008.03.001.

Archer, S. D., D. G. Cummings, C. A. Llewellyn, and J. R. Fishwick (2009), Phytoplankton taxa, irradiance and nutrient availability determine the seasonal cycle of DMSP in temperate shelf seas, *Mar. Ecol. Prog. Ser.*, *394*, 111–124, doi:10.3354/meps08284.

Archer, S. D., S. A. Kimmance, J. A. Stephens, F. E. Hopkins, R. G. J. Bellerby, K. G. Schulz, J. Piontek, and A. Engel (2013), Contrasting responses of DMS and DMSP to ocean acidification in Arctic waters, *Biogeosciences Discuss.*, *9*, 12,803–12,843, doi:10.5194/bgd-9-12803-2012.

Arrigo, K. R., and G. L. van Dijken (2004), Annual cycles of sea ice and phytoplankton in Cape Bathurst polynya, southeastern Beaufort Sea, Canadian Arctic, *Geophys. Res. Lett.*, *31*, L08304, doi:10.1029/2003GL018978.

Arrigo, K. R., et al. (2012), Massive phytoplankton blooms under Arctic Sea Ice, *Science*, *336*(6087), 1408, doi:10.1126/science.1215065.

Arrigo, K., T. Mock, and M. P. Lizotte (2010), Primary producers and sea ice, in *Sea Ice*, edited by D. N. Thomas and G. S. Dieckmann, pp. 283–325, Wiley-Blackwell, West Sussex, U. K.

Barlow, R. G., M. Gosselin, L. Legendre, J.-C. Therriault, S. Demers, R. F. C. Mantoura, and C. A. Llewellyn (1988), Photoadaptive strategies in sea-ice microalgae, *Mar. Ecol. Prog. Ser.*, *45*, 145–152, doi:10.3354/meps045145.

Bates, T. S. (1992), Sulfur emissions to the atmosphere from natural sources, *J. Atmos. Chem.*, *14*, 315–337.

Bates, S. S., and F. C. Cota (1986), Fluorescence induction and photosynthetic responses of Arctic ice algae to sample treatment and salinity, *J. Phycol.*, *70*(4), 421–429, doi:10.1111/j.1529-8817.1986.tb02484.x.

Belviso, S. (2000), Diel variations of the DMSP-to-chlorophyll *a* ratio in Northwestern Mediterranean surface waters, *J. Mar. Syst.*, *25*(2), 119–128.

Boetius, A., et al. (2013), Export of algal biomass from the melting Arctic sea ice, *Science*, *339*, 1430–1432, doi:10.1126/science.1231346.

Bouillon, R.-C., P. A. Lee, S. J. DeMora, M. Levasseur, and C. Lovejoy (2002), Vernal distribution of dimethylsulphide, dimethylsulphoniopropionate, and dimethylsulphoxide in the North Water in 1998, *Deep Sea Res., Part II*, *49*(22–23), 5171–5189, doi:10.1016/S0967-0645(02)00184-4.

Campbell, K., C. J. Mundy, D. Barber, and M. Gosselin (2014), Characterizing the sea ice algae chlorophyll *a* snow depth relationship over Arctic spring melt using transmitted irradiance, *J. Mar. Syst.*, doi:10.1016/j.jmarsys.2014.01.008, in press.

Caruana, A. M. N., M. Steinke, S. M. Turner, and G. Malin (2012), Concentrations of dimethylsulphoniopropionate and activities of dimethylsulphide-producing enzymes in batch cultures of nine dinoflagellate species, *Biogeochemistry*, *110*(1–3), 87–107, doi:10.1007/s10533-012-9705-4.

Chang, R. Y. W., S. J. Sjostedt, J. R. Pierce, T. N. Papakyriakou, M. G. Scarratt, S. Michaud, M. Levasseur, W. R. Leaitch, and J. P. D. Abbatt (2011), Relating atmospheric and oceanic DMS levels to particle nucleation events in the Canadian Arctic, *J. Geophys. Res.*, *116*, D00S03, doi:10.1029/2011JD015926.

Charlson, R. J., J. E. Lovelock, M. O. Andreae, and S. G. Warren (1987), Oceanic phytoplankton, atmospheric sulphur, cloud albedo and climate, *Nature*, *326*, 655–661, doi:10.1038/326655a0.

Cota, G. F., and C. W. Sullivan (1990), Photoadaptation, growth and production of bottom ice algae in the Antarctic, *J. Phycol.*, *26*(3), 399–411, doi:10.1111/j.0022-3646.1990.00399.x.

Cox, G. F. N., and W. F. Weeks (1983), Equations for determining the gas and brine volumes in sea-ice samples, *J. Glaciol.*, *29*(102), 306–316.

Curran, M. A. J., and G. B. Jones (2000), Dimethyl sulfide in the Southern Ocean: Seasonality and flux, *J. Geophys. Res.*, *105*(D16), 20,451–20,459, doi:10.1029/2000JD900176.

Curson, A. R. J., J. D. Todd, M. J. Sullivan, and A. W. B. Johnston (2011), Catabolism of dimethylsulphoniopropionate: Microorganisms, enzymes and genes. *Nat. Rev. Microbiol.*, *9*(12), 849–859, doi:10.1038/nrmicro2653.

Damm, E., R. P. Kiene, J. Schwarz, E. Falck, and G. S. Dieckmann (2008), Methane cycling in Arctic shelf water and its relationship with phytoplankton biomass and DMSP, *Mar. Chem.*, *109*(1–2), 45–59, doi:10.1016/j.marchem.2007.12.003.

Ehn, J. K., C. J. Mundy, D. G. Barber, H. Hop, A. Rossnagel, and J. Stewart (2011), Impact of horizontal spreading on light propagation in melt pond covered seasonal sea ice in the Canadian Arctic, *J. Geophys. Res.*, *116*, C00G02, doi:10.1029/2010JC006908.

Fortier, M., L. Fortier, C. Michel, and L. Legendre (2002), Climatic and biological forcing of the vertical flux of biogenic particles under seasonal Arctic sea ice, *Mar. Ecol. Prog. Ser.*, *225*, 1–16, doi:10.3354/meps225001.

Frey, K. E., D. K. Perovich, and B. Light (2011), The spatial distribution of solar radiation under a melting Arctic sea ice cover, *Geophys. Res. Lett.*, *38*, L22501, doi:10.1029/2011GL049421.

Gabric, J. A., B. Qu, P. Matrai, and A. C. Hirst (2005), The simulated response of dimethylsulfide production in the Arctic Ocean to global warming, *Tellus, Ser. B*, *57*(5), 391–403, doi:10.1111/j.1600-0889.2005.00163.x.

Galí, M., and R. Simó (2010), Occurrence and cycling of dimethylated sulfur compounds in the Arctic during summer receding of the ice edge, *Mar. Chem.*, *122*(1–4), 105–117, doi:10.1016/j.marchem.2010.07.003.

Garrison, D. L., and K. R. Buck (1986), Organism losses during ice melting: A serious bias in sea ice community studies, *Polar Biol.*, *6*(4), 237–239.

Gilson, G. (2010), Composition en DMS et composés soufrés associés de la glace de mer annuelle arctique en Mer de Beaufort (CFL, Canada) et implication pour les flux de DMS vers l'atmosphère, Master thesis, Univ. libre de Bruxelles, Belgium.

Golden, K. M., H. Eicken, A. L. Heaton, J. Miner, D. J. Pringle, and J. Zhu (2007), Thermal evolution of permeability and microstructure in sea ice, *Geophys. Res. Lett.*, *34*, L16501, doi:10.1029/2007GL030447.

Grasshoff, K., K. Kremling, and M. Ehrhardt (Eds.) (1999), *Methods of Seawater Analysis*, 3rd ed., Wiley-VCH, N. Y.

Griewank, P. J., and D. Notz (2014), A 1-D model study of Arctic sea-ice salinity, *The Cryosphere Discuss.*, *8*, 1723–1793, doi:10.5194/tcd-8-1723-2014.

Grøntved, J., and G. Seidenfaden (1938), The phytoplankton of the waters west of Greenland, *Medd. Groenl.*, *82*(5), 1–380.

Holm-Hansen, O., C. J. Lorenzen, R. W. Holmes, and J. D. Strickland (1965), Fluorometric determination of chlorophyll, *J. Cons. Cons. Int. Explor. Mer*, *30*, 3–15.

Howard, E. C., et al. (2006), Bacterial taxa that limit sulfur flux from the ocean, *Science*, *314*(5799), 649–652, doi:10.1126/science.1130657.

Hudier, E. J. J., R. G. Ingram, and K. Shirasawa (1995), Atmosphere-ocean upward flushing of sea water through first year ice, *Atmos. Ocean*, *33*(3), 37–41, doi:10.1080/07055900.1995.9649545.

Jones, G., D. Fortescue, S. King, G. Williams, and S. Wright (2010), Dimethylsulphide and dimethylsulphoniopropionate in the South-West Indian Ocean sector of East Antarctica from 301 to 801E during BROKE-West, *Deep-Sea Res., Part II*, *57*, 863–876, doi:10.1016/j.dsr2.2009.01.003.

Juhl, A., and C. Krembs (2010), Effects of snow removal and algal photoacclimation on growth and export of ice algae, *Polar Biol.*, *33*, 1057–1065, doi:10.1007/s00300-010-0784-1.

Kasamatsu, N., T. Hirano, T. Odate, and M. Fukuchi (2004), Dimethylsulfoniopropionate production by psychrophilic diatom isolates, *J. Phycol.*, *40*, 874–878, doi:10.1111/j.1529-8817.2004.03122.x.

Keller, M. D., W. K. Bellows, and R. R. L. Guillard (1989), Dimethylsulfide production in marine phytoplankton, in *Biogenic Sulfur in the Environment*, edited by E. S. Saltzman and W. J. Cooper, pp. 167–182, Am. Chem. Soc., Washington, D. C.

Kettle, A. J., and M. O. Andreae (2000), Flux of dimethylsulfide from the oceans: A comparison of updated data sets and flux models, *J. Geophys. Res.*, *105*(D22), 26,793–26,808, doi:10.1029/2000JD900252.

Kiene, R. P., and D. Slezak (2006), Low dissolved DMSP concentrations in seawater revealed by small-volume gravity filtration and dialysis sampling, *Limnol. Oceanogr. Methods*, *4*, 80–95.

Kiene, R. P., L. J. Linn, and J. A. Bruton (2000), New and important roles for DMSP in marine microbial communities, *J. Sea Res.*, *43*(3–4), 209–224, doi:10.1016/S1385-1101(00)00023-X.

Kiene, R. P., D. J. Kieber, D. Slezak, D. A. Toole, D. A. del Valle, J. Bisgrove, J. Brinkley, and A. Rellinger (2007), Distribution and cycling of dimethylsulfide, dimethylsulfoniopropionate, and dimethylsulfoxide during spring and early summer in the Southern Ocean south of New Zealand, *Aquat. Sci.*, *69*, 305–319, doi:10.1007/s00027-007-0892-3.

Kirst, G. O., C. Thiel, H. Wolff, J. Nothnagel, M. Wanzek, and R. Ulmke (1991), Dimethylsulfoniopropionate (DMSP) in ice-algae and its possible biological role, *Mar. Chem.*, *35*(1–4), 381–388, doi:10.1016/S0304-4203(09)90030-5.

Laroche, D., A. F. Vézina, M. Levasseur, M. Gosselin, J. Stefels, M. D. Keller, P. A. Matrai, and R. L. J. Kwint (1999), DMSP synthesis and exudation in phytoplankton: A modeling approach, *Mar. Ecol. Prog. Ser.*, *180*, 37–49, doi:10.3354/meps180037.

Lavoie, D., K. L. Denman, and C. Michel (2005), Modeling ice algal growth and decline in a seasonally ice-covered region of the Arctic (Resolute Passage, Canadian Archipelago), *J. Geophys. Res.*, *110*, C11009, doi:10.1029/2005JC002922.

Lee, P. A., S. J. De Mora, M. Gosselin, M. Levasseur, R.-C. Bouillon, C. Nozais, and C. Michel (2001), Particulate dimethylsulfoxide in Arctic sea-ice algal communities: The cryoprotectant hypothesis revisited, *J. Phycol.*, *37*(4), 488–499, doi:10.1046/j.1529-8817.2001.037004488.x.

Lee, P. A., P. A. Sanders, S. J. De Mora, D. Deibel, and M. Levasseur (2003), Influence of copepod grazing on concentrations of dissolved dimethylsulfoxide and related sulfur compounds in the North Water, northern Baffin Bay, *Mar. Ecol. Prog. Ser.*, *255*, 235–248, doi:10.3354/meps255235.

Lee, P. A., S. F. Riseman, C. E. Hare, A. David, K. Leblanc, and G. R. DiTullio (2011), Potential impact of increased temperature and CO_2 on particulate dimethylsulfoniopropionate in the Southeastern Bering Sea, *Adv. Oceanogr. Limnol.*, *2*(1), 33–47, doi:10.1080/19475721.2011.574433.

Levasseur, M. (2013), The Arctic meltdown and the microbial cycling of sulphur, *Nat. Geosci.*, *6*, 691–700, doi:10.1038/NGEO1910.

Levasseur, M., M. Gosselin, and S. Michaud (1994), A new source of dimethylsulfide (DMS) for the arctic atmosphere: Ice diatoms, *Mar. Biol.*, *121*(2), 381–387, doi:10.1007/BF00346748.

Lizotte, M. P. (2003), The microbiology of sea ice, in *Sea Ice: An Introduction to its Physics, Chemistry, Biology and Geology*, edited by D. N. Thomas and G. S. Dieckmann, pp. 184–210, Blackwell Sci., Oxford, U. K.

Luce, M., et al. (2011), Distribution and microbial metabolism of dimethylsulfoniopropionate and dimethylsulfide during the 2007 Arctic ice minimum, *J. Geophys. Res.*, *116*, C00G06, doi:10.1029/2010JC006914.

Lund, J. W. G., C. Kipling, and E. D. Le Cren (1958), The inverted microscope method of estimating algal number and the statistical basis of estimations by counting, *Hydrobiologia*, *11*, 143–170, doi:10.1007/BF00007865.

Martin, J., J.-É. Tremblay, J. Gagnon, G. Tremblay, A. Lapoussière, C. Jose, M. Poulin, M. Gosselin, Y. Gratton, and C. Michel (2010), Prevalence, structure and properties of subsurface chlorophyll maxima in Canadian Arctic waters, *Mar. Ecol. Prog. Ser.*, *412*, 69–84, doi:10.3354/meps08666.

Matrai, P., and S. Apollonio (2013), New estimates of microalgae production based upon nitrate reductions under sea ice in Canadian shelf seas and the Canada Basin of the Arctic Ocean, *Mar. Biol.*, *160*, 1297–1309, doi:10.1007/s00227-013-2181-0.

Matrai, P. A., and M. Vernet (1997), Dynamics of the vernal bloom in the marginal ice zone of the Barents Sea: Dimethyl sulfide and dimethylsulfoniopropionate budgets, *J. Geophys. Res.*, *102*(C10), 22,965–22,979, doi:10.1029/96JC03870.

Matrai, P. A., M. Vernet, R. Hood, A. Jennings, E. Brody, and S. Saemundsdottir (1995), Light-dependence of carbon and sulfur production by polar clones of the genus *Phaeocystis*, *Mar. Biol.*, *124*(1), 157–167, doi:10.1007/BF00349157.

Matrai, P. A., M. Vernet, and P. Wassmann (2007), Relating temporal and spatial patterns of DMSP in the Barents Sea to phytoplankton biomass and productivity, *J. Mar. Syst.*, *67*(1–2), 83–101, doi:10.1016/j.jmarsys.2006.10.001.

Matrai, P. A., L. Tranvik, C. Leck, and J. C. Knulst (2008), Are high Arctic surface microlayers a potential source of aerosol organic precursors?, *Mar. Chem.*, *108*, 109–122, doi:10.1016/j.marchem.2007.11.001.

Michel, C., L. Legendre, S. Demers, and J.-C. Therriault (1988), Photoadaptation of sea-ice microalgae in springtime: Photosynthesis and carboxylating enzymes, *Mar. Ecol. Prog. Ser.*, *50*, 177–185.

Mikkelsen, D. M., and A. Witkowski (2010), Melting sea ice for taxonomic analysis: A comparison of four melting procedures, *Polar Res.*, *29*(3), 451–454, doi:10.1111/j.1751-8369.2010.00162.x.

Modini, R. L., Z. D. Ristovski, G. R. Jognson, C. He, N. Surawski, L. Morawska, T. Suni, and M. Kulmala (2009), New particle formation and growth at a remote, sub-tropical coastal location, *Atmos. Chem. Phys. Discuss.*, *9*, 12,101–12,139, doi:10.5194/acp-9-7607-2009.

Moran, M. A., C. R. Reisch, R. P. Kiene, and W. B. Whitman (2012), Genomic insights into bacterial DMSP transformations, *Annu. Rev. Mar. Sci.*, *4*(1), 523–542, doi:10.1146/annurev-marine-120710-100827.

Motard-Côté, J., et al. (2012), Distribution and metabolism of dimethylsulfoniopropionate (DMSP) and phylogenetic affiliation of DMSP-assimilating bacteria in northern Baffin Bay/Lancaster Sound, *J. Geophys. Res.*, *117*, C00G11, doi:10.1029/2011JC007330.

Mundy, C. J., D. G. Barber, and C. Michel (2005), Variability of snow and ice thermal, physical and optical properties pertinent to sea ice algae biomass during spring, *J. Mar. Syst.*, *58*, 107–120.

Mundy, C. J., et al. (2009), Contribution of under-ice primary production to an ice-edge upwelling phytoplankton bloom in the Canadian Beaufort Sea, *Geophys. Res. Lett.*, *36*, L17601, doi:10.1029/2009GL038837.

Mundy, C. J., M. Gosselin, Y. Gratton, K. Brown, V. Galindo, K. Campbell, M. Levasseur, D. Barber, T. Papakyriakou, and S. Bélanger (2014), Role of environmental factors on phytoplankton bloom initiation under landfast sea ice in Resolute Passage, Canada, *Mar. Ecol. Prog. Ser.*, *497*, 39–49, doi:10.3354/meps10587.

Nicolaus, M., C. Katlein, J. Maslanik, and S. Hendricks (2012), Changes in Arctic sea ice result in increasing light transmittance and absorption, *Geophys. Res. Lett.*, *39*, L24501, doi:10.1029/2012GL053738.

Nomura, D., N. Kasamatsu, K. Tateyama, S. Kudoh, and M. Fukuchi (2011), DMSP and DMS in coastal fast ice and under-ice water of Lützow-Holm Bay, eastern Antarctica, *Cont. Shelf Res.*, *31*(13), 1377–1383, doi:10.1016/j.csr.2011.05.017.

Parsons, T. R., Y. Maita, and C. M. Lalli (1984), *A Manual of Chemical and Biological Methods for Seawater Analysis*, Pergamon, New York.

Perovich, D. K., B. Light, H. Eicken, K. F. Jones, K. Runciman, and S. V. Nghiem (2007), Increasing solar heating of the Arctic Ocean and adjacent seas, 1979–2005: Attribution and role in the ice-albedo feedback, *Geophys. Res. Lett.*, *34*, L19505, doi:10.1029/2007GL031480.

Petrich, C., and H. Eicken (2010), Growth, structure and properties of sea ice, in *Sea Ice*, 2nd ed., edited by D. N. Thomas and G. S. Dieckmann, pp. 23–77, Wiley-Blackwell, West Sussex, U. K.

Popova, E. E., A. Yool, A. C. Coward, Y. K. Aksenov, S. G. Alderson, B. A. de Cuevas, and T. R. Anderson (2010), Control of primary production in the Arctic by nutrients and light: Insights from a high resolution ocean general circulation model, *Biogeosciences*, *7*, 3569–3591, doi:10.5194/bg-7-3569-2010.

Poulin, M., N. Daugbjerg, R. Gradinger, L. Ilyash, T. Ratkova, and C. von Quillfeldt (2011), The pan-Arctic biodiversity of marine pelagic and sea-ice unicellular eukaryotes: A first-attempt assessment, *Mar. Biodiversity*, *41*, 13–28, doi:10.1007/s12526-010-0058-8.

Pringle, D. J., J. E. Miner, H. Eicken, and K. M. Golden (2009), Pore space percolation in sea ice single crystals, *J. Geophys. Res.*, *114*, C12017, doi:10.1029/2008JC005145.

Qu, B., and A. J. Gabric (2010), Using genetic algorithms to calibrate a dimethylsulfide production model in the Arctic Ocean, *Chin. J. Oceanol. Limnol.*, *28*(3), 573–582, doi:10.1007/s00343-010-9062-x.

Quinn, P. K., and T. S. Bates (2011), The case against climate regulation via oceanic phytoplankton sulphur emissions, *Nature*, *480*(7375), 51–56, doi:10.1038/nature10580.

Rawlins, M. A., et al. (2010), Analysis of the Arctic system for freshwater cycle intensification: Observations and expectations, *J. Clim.*, *23*, 5715–5737, doi:10.1175/2010JCLI3421.1.

Rempillo, O., et al. (2011), Dimethyl sulfide air-sea fluxes and biogenic sulfur as a source of new aerosols in the Arctic fall, *J. Geophys. Res.*, *116*, D00S04, doi:10.1029/2011JD016336.

Royer, S.-J., et al. (2010), Microbial dimethylsulfoniopropionate (DMSP) dynamics along a natural iron gradient in the northeast subarctic Pacific, *Limnol. Oceanogr. Methods*, *55*(4), 1614–1626, doi:10.4319/lo.2010.55.4.1614.

Scarratt, M. G., M. Levasseur, S. Michaud, G. Cantin, M. Gosselin, and S. J. De Mora (2002), Influence of phytoplankton taxonomic profile on the distribution of dimethylsulfide and dimethylsulfoniopropionate in the northwest Atlantic, *Mar. Ecol. Prog. Ser.*, *244*, 49–61.

Schlitzer, R. (2010), *Ocean Data View*, Alfred Inst. for Polar and Mar. Res., Bremerhaven, Germany. [Available at http://odv.awi.de.]

Simó, R. (2001), Production of atmospheric sulfur by oceanic plankton: Biogeochemical, ecological and evolutionary links, *Trends Ecol. Evol.*, *16*(6), 287–294.

Smith, R. E. H., P. C. Anning, and G. Cota (1988), Abundance and production of ice algae n Resolute Passage, Canadian Arctic, *Mar. Ecol. Prog. Ser.*, *48*, 251–263.

Sokal, R. R., and F. J. Rohlf (1995), *Biometry: The Principles and Practice of Statistics in Biological Research*, 3rd ed., W. H. Freeman, New York.

Stefels, J. (2000), Physiological aspects of the production and conversion of DMSP in marine algae and higher plants, *J. Sea Res.*, *43*(3–4), 183–197, doi:10.1016/S1385-1101(00)00030-7.

Stefels, J., M. Steinke, S. M. Turner, G. Malin, and S. Belviso (2007), Environmental constraints on the production and removal of the climatically active gas dimethylsulphide (DMS) and implications for ecosystem modeling, *Biogeochemistry*, *83*(1–3), 245–275, doi:10.1007/s10533-007-9091-5.

Stefels, J., G. Carnat, J. W. H. Dacey, T. Goossens, J. T. M. Elzenga, and J.-L. Tison (2012), The analysis of dimethylsulfide and dimethylsulfoniopropionate in sea ice: Dry-crushing and melting using stable isotope additions, *Mar. Chem.*, *128–129*, 34–43, doi:10.1016/j.marchem.2011.09.007.

Steinke, M., G. Malin, S. W. Gibb, and P. H. Burkill (2002), Vertical and temporal variability of DMSP lyase activity in a coccolithophorid bloom in the northern North Sea, *Deep Sea Res., Part II*, *49*(15), 3001–3016, doi:10.1016/S0967-0645(02)00068-1.

Sunda, W., D. J. J. Kieber, R. P. Kiene, and S. Huntsman (2002), An antioxidant function for DMSP and DMS in marine algae, *Nature*, *418*(6895), 317–320, doi:10.1038/nature00851.

Thomas, D. N., and S. Papadimitriou (2003), Biogeochemistry of sea ice, in *Sea Ice: An Introduction to its Physics, Biology, Chemistry and Geology*, edited by D. N. Thomas and G. S. Dieckmann, pp. 267–302, Blackwell Sci., Oxford, U. K.

Timco, G. W., and R. M. W. Frederking (1996), A review of sea ice density, *Cold Reg. Sci. Technol.*, *24*, 1–6.

Tison, J. L., F. Brabant, I. Dumont, and J. Stefels (2010), High-resolution dimethyl sulfide and dimethylsulfoniopropionate time series profiles in decaying summer first-year sea ice at Ice Station Polarstern, western Weddell Sea, Antarctica, *J. Geophys. Res.*, *115*, G04044, doi: 10.1029/2010JG001427.

Tremblay, J.-É., K. Simpson, J. Martin, L. Miller, Y. Gratton, D. Barber, and N. M. Price (2008), Vertical stability and the annual dynamics of nutrients and chlorophyll fluorescence in the coastal, southeast Beaufort Sea, *J. Geophys. Res.*, *113*, C07S90, doi:10.1029/2007JC004547.

Trevena, A. J., and G. Jones (2006), Dimethylsulphide and dimethylsulphoniopropionate in Antarctic sea ice and their release during sea ice melting, *Mar. Chem.*, *98*(2–4), 210–222, doi:10.1016/j.marchem.2005.09.005.

Trevena, A. J., and G. Jones (2012), DMS flux over the Antarctic sea ice zone, *Mar. Chem.*, *134–135*, 45–58, doi:10.1016/j.marchem.2012.03.001.

Trevena, A. J., G. B. Jones, S. W. Wright, and R. L. van den Enden (2003), Profiles of dimethylsulfoniopropionate (DMSP), algal pigments, nutrients, and salinity in the fast ice of Prydz Bay, Antarctica, *J. Geophys. Res.*, *108*(C5), 3145, doi:10.1029/2002JC001369.

Turner, S. M., G. Malin, P. S. Liss, D. S. Harbour, and P. M. Holligan (1988), The seasonal variation of dimethylsulfide and dimethylsulfoniopropionate concentrations in nearshore waters, *Limnol. Oceanogr.*, *33*(3), 364–375, doi:10.4319/lo.1988.33.3.0364.

Uzuka, N. A. (2003), A time series observation of DMSP production in the fast ice zone near Barrow, *Tohoku Geophys. J.*, *36*(4), 439–442.

Vairavamurthy, A., M. O. Andreae, and R. L. Iverson (1985), Biosynthesis of dimethylsulfide and dimethylpropiothetin by *Hymenomonas carterae* in relation to sulfur source and salinity variations, *Limnol. Oceanogr.*, *30*(1), 59–70.

Van Rijssel, M., and W. W. C. Gieskes (2002), Temperature, light, and the dimethylsulfoniopropionate (DMSP) content of *Emiliania huxleyi* (Prymnesiophyceae), *J. Sea Res.*, *48*, 17–27, doi:10.1016/S1385-1101(02)00134-X.

Vancoppenolle, M., H. Goosse, A. de Montety, T. Fichefet, B. Tremblay, and J.-L. Tison (2010), Modeling brine and nutrient dynamics in Antarctic sea ice: The case of dissolved silica, *J. Geophys. Res.*, *115*, C02005, doi:10.1029/2009JC005369.

Vancoppenolle, M., C. M. Bitz, and T. Fichefet (2007), Summer landfast sea ice desalination at Point Barrow, Alaska: Modeling and observations, *J. Geophys. Res.*, *112*, C04022, doi:10.1029/2006JC003493.

Vila-Costa, M., R. Simó, L. Alonso-Sáez, and C. Pedrós-Alió (2008), Number and phylogenetic affiliation of bacteria assimilating dimethylsulfoniopropionate and leucine in the ice-covered coastal Arctic Ocean, *J. Mar. Syst.*, *74*(3–4), 957–963, doi:10.1016/j.jmarsys.2007.10.006.

von Quillfeldt, C. H. (2000), Common diatom species in arctic spring blooms: Their distribution and abundance, *Bot. Mar.*, *43*, 499–516, doi: 10.1515/BOT.2000.050.

White, D., et al. (2007), The arctic freshwater system: Changes and impacts, *J. Geophys. Res.*, *112*, G04S54, doi:10.1029/2006JG000353.

Wolfe, G. V., M. Steinke, and G. O. Kirst (1997), Grazing-activated chemical defense in a unicellular marine alga, *Nature*, *387*, 894–897.

Zeebe, R. E., H. Eicken, D. H. Robinson, D. Wolf-Gladrow, and G. S. Dieckmann (1996), Modeling the heating and melting of sea ice through light absorption by microalgae, *J. Geophys. Res.*, *101*(C1), 1163–1181.

Zhang, J., R. Lindsay, M. Steele, and A. Schweiger (2008), What drove the dramatic retreat of arctic sea ice during summer 2007?, *Geophys. Res. Lett.*, *35*, L11505, doi:10.1029/2008GL034005.

Zhang, X. (2010), Sensitivity of arctic summer sea ice coverage to global warming forcing: Towards reducing uncertainty in Arctic climate change projections, *Tellus, Ser. A*, *62*(3), 220–227, doi:10.1111/j.1600-0870.2010.00441.x.